METALLOGENY OF A VOLCANOGENIC GOLD DEPOSIT, CAPE ST. JOHN GROUP, TILT COVE, NEWFOUNDLAND

METALLOGENY OF A VOLCANOGENIC GOLD DEPOSIT, CAPE ST. JOHN GROUP, TILT COVE, NEWFOUNDLAND

By

TRACY D. HURLEY

A Thesis

Submitted to the Department of Geology

in Partial Fulfillment of the Requirements

for the Degree

Batchelor of Science

McMaster University

April, 1982

BATCHELOR OF SCIENCE (1982)

(Geology)

McMASTER UNIVERSITY
HAMILTON, ONTARIO

Title : Metallogeny of a volcanogenic gold deposit, Cape St. John Group, Tilt Cove, Newfoundland.

Author : Tracy D. Hurley

Supervisor : Dr. James H. Crocket

Number of pages : ix , 69

ABSTRACT

The "B" horizon at Tilt Cove occurs in subaqueous mafic volcanics near the base of the Silurian Cape St. John Group It is 3 metres below a well-banded oxide iron formation ("A" horizon).

Mineralization in the "B" horizon is analogous to that of the East Mine in that it is volcanogenic and has resulted in extensive chloritization of the footwall rocks, and in the deposition of banded sulphides or the replacement of the existing mafic volcanics by sulphides. There are differences in the geochemistry mineral textures and mineral types. The East Mine host volcanics are alkali depleted basaltic komatiites to magnesium theleiites. The "B" horizon host volcanics are spillitized magnesium tholeiites. Samples of ore from the East Mine show well-developed colloform and framboidal textures. Pyrite, magnetite, hematite and chalcopyrite are the dominant minerals with minor sphalerite and accessory covellite. Samples from the "B" horizon show relict colloform textures and framboids with less internal structure due to overgrowths. Atoll textures indicating extensive replacement are common. Pyrite is the dominant sulphide followed by sphalerite, chalcopyrite, accessory covellite and gold. The chalcopyrite occurs both as replacement of pyrite and exsolution in sphalerite. The most significant difference between samples from the East Mine and "B" horizon is the greater abundance of gold in the "B" horizon and its correlation with sphalerite.

ACKNOWLEDGEMENTS

The author wishes to thank Newmont Exploration of Canada Ltd., for their assistance and co-operation which made this thesis possible.

For initiating this project and introducing me to the area I sincerely thank Richard T. Kusmirski. Thanks must also go to Richard T. Kusmirski and Andrew Fyon for their valuable suggestions.

I express my appreciation to Dr. J.H. Crocket for his supervision of this thesis.

For assistance in activation analysis and chemical analyses of rocks I thank Abdul Kabir and Otto Mudroch respectively. To Len Zwicker for his preparation of thin sections and Jack Whorwood for his preparation of photographs, I also extend my appreciation. J.V. Hurley was kind enough to type the manuscript, however, I am no longer welcome at home.

Finally I would like to thank Joe Cow and the graduating class of 1982, for making this a truly memorable year.

TABLE OF CONTENTS

LIST OF PLATES

LIST OF FIGURES

LIST OF TABLES

CHAPTER 1

INTRODUCTION

1.1 LOCATION AND ACCESSIBILITY

The study area lies immediately notheast of Tilt Cove within claim blocks owned by Newmont Exploration of Canada Ltd. Tilt Cove lies in the eastern end of the Burlington (Baie Verte) Peninsula, Newfoundland (Figure 1). The outport is largely abandoned with only 15 families remaining, the inhabitants being fishermen and employees of Rambler Consolidated Mines Ltd. As illustrated in Plate 1, Tilt Cove consists essentially of a large circular pond surrounded on three sides by high vertical cliffs, the fourth side leading out to the ocean. It is geographically located 200 km northeast of Deer Lake and 230 km northwest of Gander. An airport is present in each town. Access to Tilt Cove from either town is via highways and gravel roads.

1.2 HISTORICAL BACKGROUND

Copper was first discovered at Tilt Cove in 1857. From 1864 to 1917 approxiamately 61,000 short tons of Cu were recovered from 1.5 million tons of ore grading at 4% to 12% Cu. A small nickel ore body containing nickel arsenides, arsenopyrite and millerite was mined between 1869 and 1876. The Tilt Cove Mine was re-opened between 1957 and 1967 by First Maritime Mining Corporation. An estimated 90,000 short tons of Cu and 42,000 ounces of Au were recovered from 7.4 million tons of ore.

Most of the ore came from the East Mine which now consists of

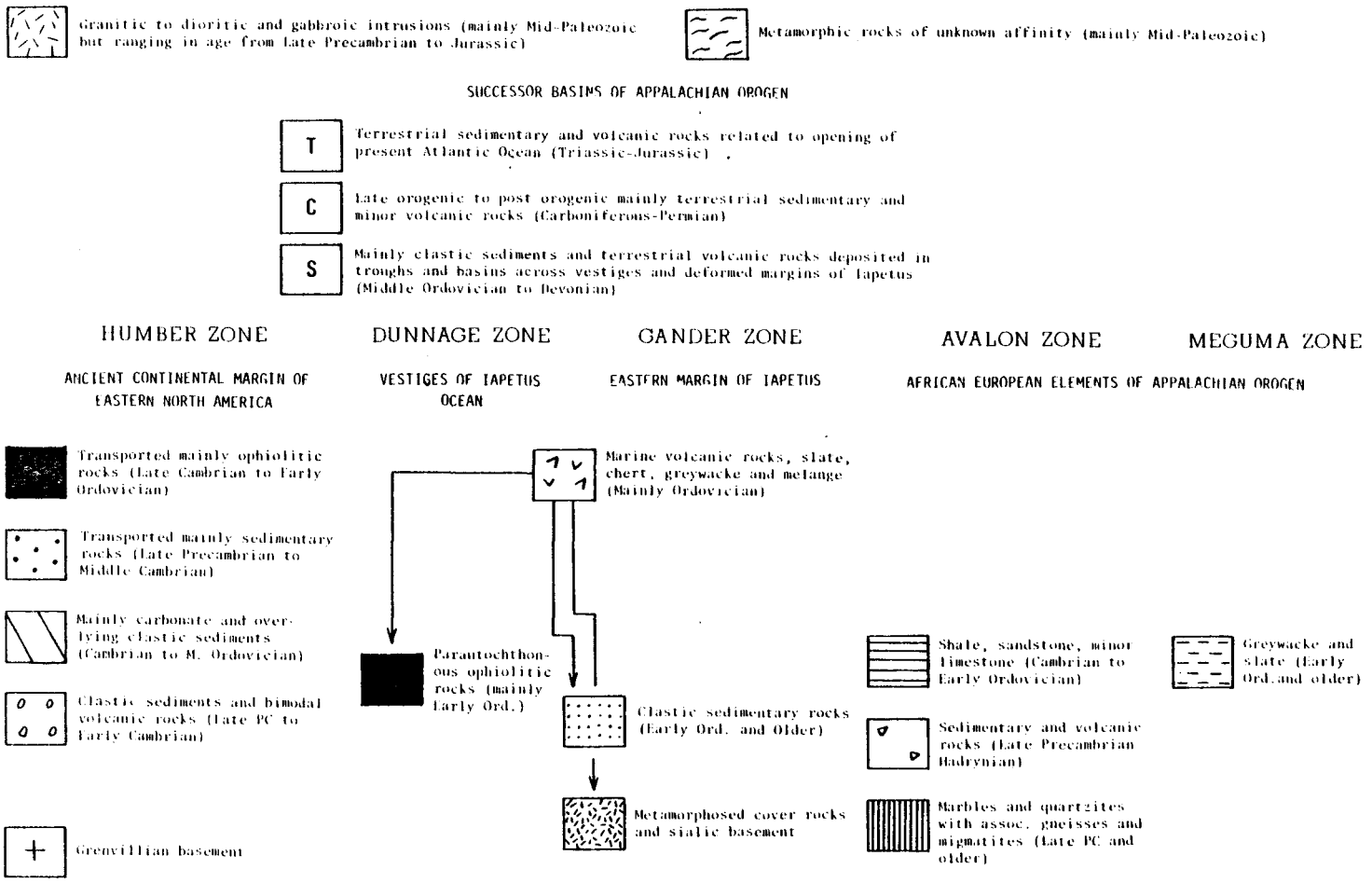

FIGURE 1. Location of Tilt Cove and general geology of Newfoundland. From Williams (1979).

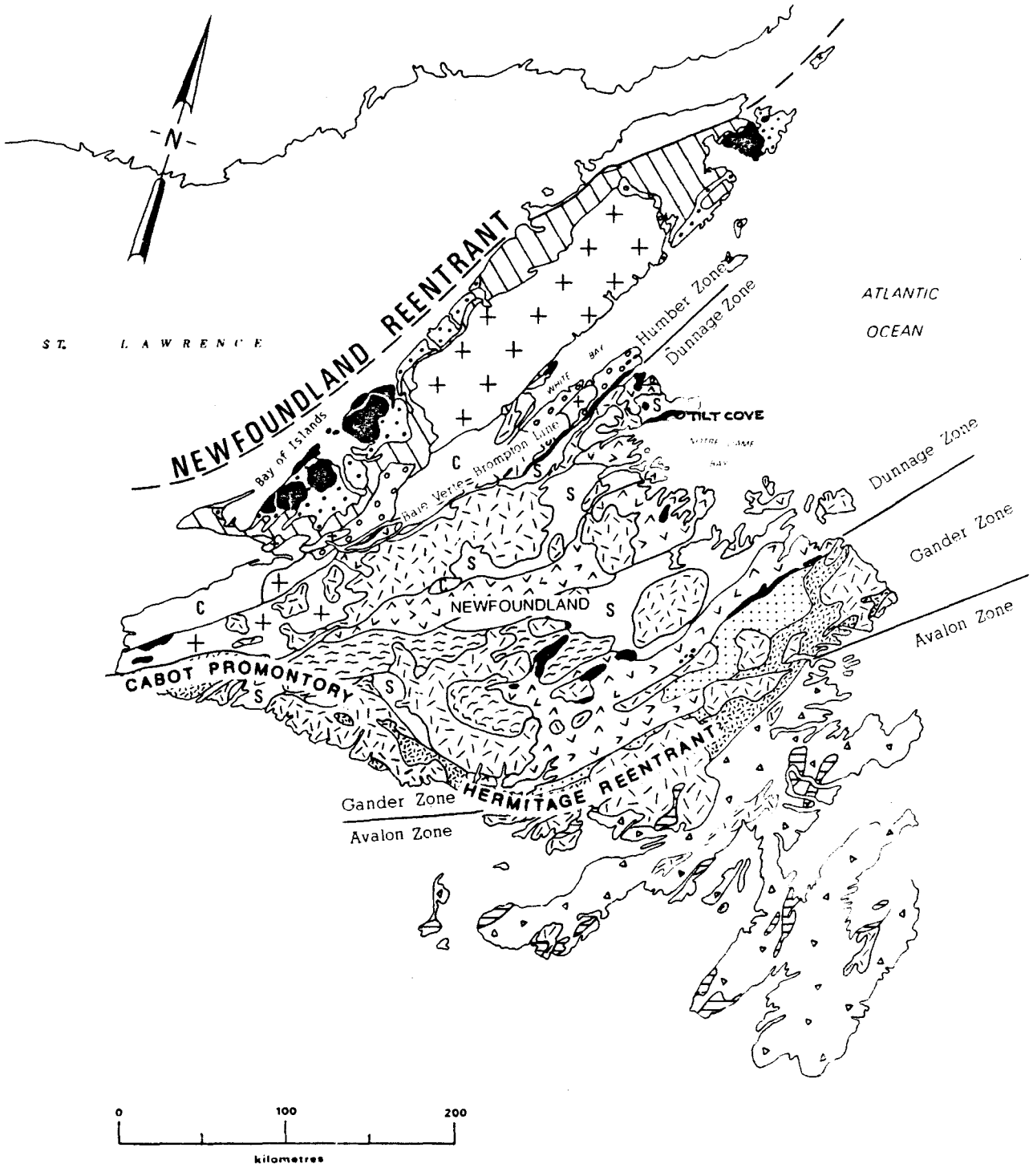
N
ST. LAWRENCE
ATLANTIC
OCEAN
NEWFOUNDLAND REENTRANT
Bay of Islands
Humber Zone
Dunnage Zone
TILT COVE
Baie Verte-Brompton Line
Dunnage Zone
Gander Zone
Avalon Zone
NEWFOUNDLAND
CABOT PROMONTORY
HERMITAGE REENTRANT
Gander Zone
Avalon Zone
0
100
200
kilometres

PLATE 1. Downtown Tilt Cove. Ocean frontage and beach resort to left.

several large open pits from collapse (Plate 2). The West Mine is a continuation of ore bodies from the East Mine. The shaft and numerous adits were blown out when the mine was closed leaving a large open pit (Plate 3).

1.3 STATEMENT OF PROBLEM

The purpose of this thesis is to determine the mineral paragenesis of a previously untested sulphide zone and compare and contrast it with the East Mine mineralization. The host volcanics will be characterized geochemically and petrograhically, and an attempt to discern the origin of the gold will be made. The samples were collected in the fall of 1981.

PLATE 2. East Mine. Open pits and talus, Tilt Cove, Nfld.

PLATE 3. West Mine. Collapsed shaft and adits.

CHAPTER 2

GENERAL GEOLOGY

2.1 PREVIOUS WORK

2.1.1 Snooks Arm Group

Tilt Cove lies at the northern end of a 16 Km long arcuate belt of rocks (Figure 2). The Betts Cove ophiolite lies at the southern end. The entire belt has been interpreted by previous authors (Church and Stevens, 1970, 1971, ; Upadhyay et al., 1971 ; Upadhyay and Neale, 1976 ; De Grace et al., 1976) as a continuous ophiolitic suite. Upadhyay (1973) described the geology in detail. On a tectonic map of Newfoundland the rocks lie within the Dunnage Zone and are considered to be vestiges of the Lower Ordivician Proto-Atlantic Ocean, Iapetus (Williams, 1979).

The basal part of the Snooks Arm Group, exposed at both Tilt Cove and Betts Cove, has been interpreted as oceanic crust overlain by island arc volcanic and sedimentary rocks (Upadhyay et al., 1971 ; Upadhyay and Neale, 1976 ; Strong, 1977). These rocks are conformably overlain by four sedimentary and volcanic units which are considered representative of a marginal basin or ocean island environment (Jenner and Fryer, 1980). All of the formations face south and occupy the north limb of a slightly overturned, easterly plunging syncline (Upadhyay, 1973 ; Neale et al , 1975).

The most recent work in the Tilt Cove area was carried out under contract for Newmont Exploration of Canada Ltd. by Strong (1980), and Kusmirski and Norman (1981).

FIGURE 2. Geology of Betts Cove - Tilt Cove after De Grace et al. (1976).

LEGEND

Silurian

CBP - Cape Brule porphyry.

P - quartz-feldspar porphyry.

CAPE ST. JOHN GROUP

C - silicic and mafic lavas, pyroclastics, subaerial and subaqueous sediments, silicic porphyries.

Ordivician

SNOOKS ARM GROUP

9 - Round Harbour Basalt; pillow lava, diabase dykes and sills.

8 - Balsam Bud Formation; sedimentary rocks, subordinate pyroclastic rocks, diabase dykes and sills, minor pillow lava.

7 - Venams Bight Basalt; pillow lava, diabase dykes and sills, minor pillow breccia.

6 - Bobby Cove Formation; sedimentary and pyroclastic rocks, diabase dykes and sills, minor pillow lavas.

4 - pillow lava, minor pillow breccia and sedimentary rocks.

3 - sheeted dykes.

2 - gabbro, commonly layered.

1 - Ultramafic, well-layered at Betts Cove.

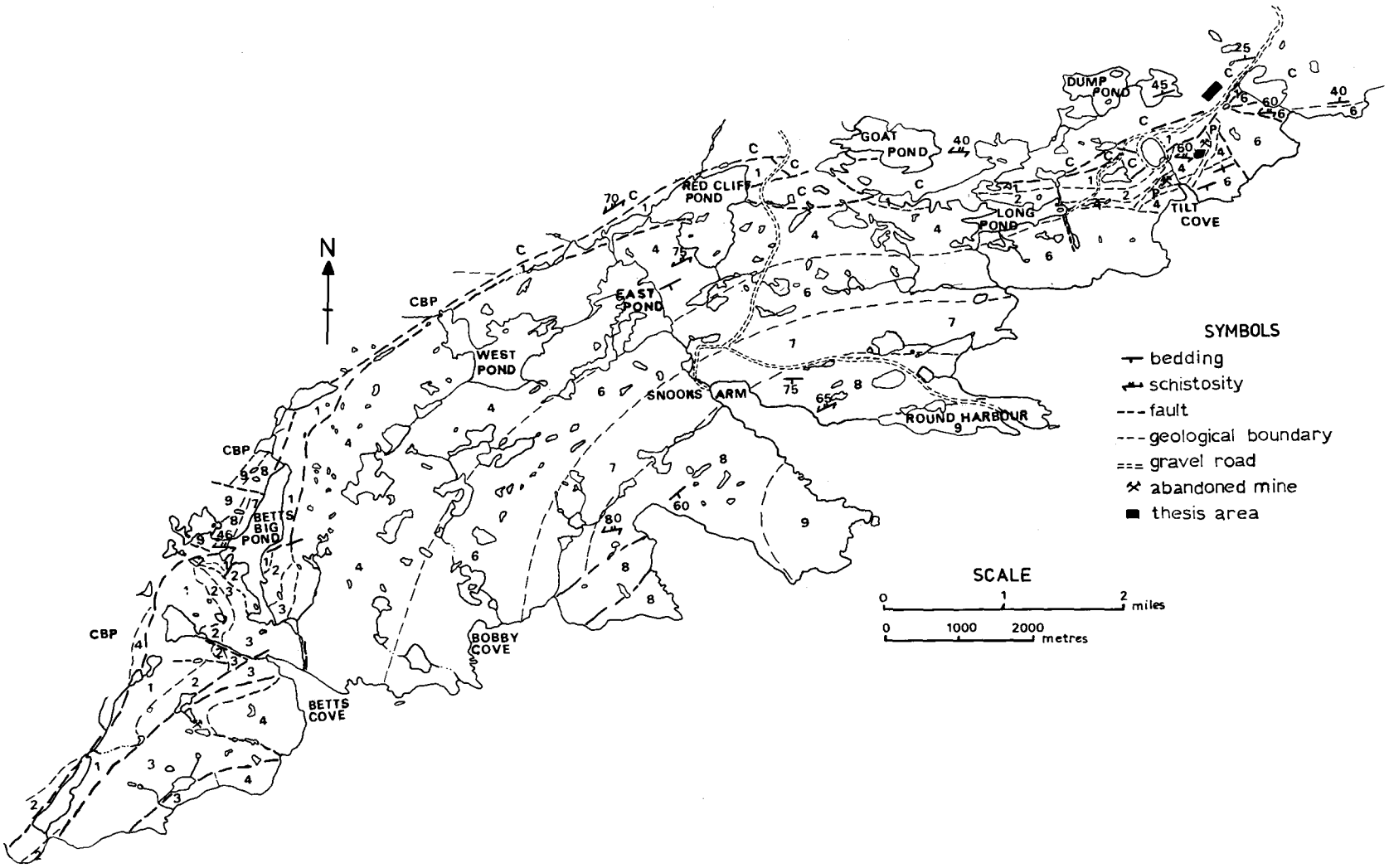
N
CBP
CBP
CBP
WEST POND
EAST POND
RED CLIFF POND
GOAT POND
DUMP POND
LONG POND
TILT COVE
SNOOKS ARM
ROUND HARBOUR
BETTS BIG POND
BETTS COVE
BOBBY COVE
SYMBOLS
bedding
schistosity
fault
geological boundary
gravel road
abandoned mine
thesis area
SCALE
0 1 2 miles
0 1000 2000 metres

2.1.2 Cape St. John Group

The Cape St. John Group consists of silicic and mafic lavas and associated pyroclastics, subaerial and subaqueous sediments, and silicic porphyries (Neale et al., 1975 ; Kusmirski and Norman, 1981).

The age of the rocks is contentious. They were first named by Baird (1951) who considered the Cape St. John Group to conformably overlie the Snooks Arm Group. Neale (1957) suggested a Devonian age for the rocks and an unconformable contact with the underlying Snooks Arm Group. Church (1965), and Neale and Kennedy (1967) agreed on an unconformable contact but suggested a Silurian age for the rocks. Dewey and Bird (1971) speculated that the Cape St. John Group was older than the Snooks Group and formed part of the pre-Ordivician Fleur de Lys Supergroup. This view is contested by Neale et al. (1975), De Grace et al. (1976), and Kusmirski and Norman (1981) who use field evidence to support their theory that the Cape St. John Group is Silurian in age and unconformably overlies the Snooks Arm Group.

2.2 GEOLOGY OF TILT COVE

The thesis area lies to the east of Tilt Cove. The geology of the area is as follows: - the Snooks Arm Group trends northeast and dips and faces southeast towards the ocean. The group consists of a basal, generally serpentinized ultramafic rock which outcrops along the road to Tilt Cove. The ultramafics are succeeded by a sequence of commonly variolitic mafic pillow volcanics and pillow breccia which in turn is overlain by gray and red argillaceous sediments and iron formations. The mafic volcanic through iron formation sequence is intruded by quartz-feldspar porphyries. Much of the Tilt Cove area is affected by late, normal faulting.

The East Mine occurs within the mafic sequence. Mineralization as exposed on the surface is commonly within pillow breccia and occassionaly pillow salvages. Some massive sulphide zones were observed in the open pits. According to Donoghue et al. (1959) both massive sulphide zones and stock-work bodies were mined at depth. The shape of these ore bodies is roughly lenticular and their attitudes are steeply dipping, parallel to the local schistosity. Both float and in-situ samples were obtained from the East Mine.

The Cape St. John Group outcrops north of the Tilt Cove Road. The sequence consists of variolitic pillow volcanics (Plate 4) with minor inter-pillow sediment conformably overlain by medium to course-grained calcareous sediments, agglomerates, subaerial vesicular basalts and locally fine-grained, finely laminated sediments. It strikes northeast and dips sub-horizontally to appoxiamately 40° to the northwest.

Both the "A" and "B" horizons occur within the mafic volcanics (Plates 5 and 6). The "B" horizon is stratiform and outcrops at two locales. It is up to 2 metres in thickness and has a known strike length of 150 metres (Kusmirski and Norman, 1981). In the studied locality (eastern end) it is attentuated by a fault to the east and talus to the west. Removal of overburden revealed a heavily gossaned zone (Plate 7). Pillow and pillow breccia textures are still easily recognizable (Plates 8 and 9). It is common for the pillows and fragments to be completely replaced by sulphides (Plates 10 and 11). Near the top of the zone the sulphides are commonly banded (Plates 12 and 13) although fragmental textures are still evident (Plate 14). Approxiamately 3 metres above the "B" horizon is an oxide ± chert well-banded iron formation designated the "A" horizon. It is 1 to 2 metres thick with a known strike of 160 metres. The formation consists

PLATE 4. Variolitic pillowed volcanics, from sample TDH-43, Cape St. John Group.

PLATE 5. View of "A" and "B" horizons (as indicated) from Tilt Cove Road.


CM 1 2 3 4 5 6 7 8 9 10 11


A
B

PLATE 6. View of "A" and "B" horizons (as indicated) from talus slope.

PLATE 7. Heavily gossaned "B" horizon, looking west.

PLATE 8. Well-developed pillow structures in gossaned "B" horizon.

PLATE 9. Pillow and pillow breccia replaced by sulphides, "B" horizon.


Nikon

PLATE 10. Complete replacement of pillow by sulphides, "B" horizon.

PLATE 11. Complete replacement of pillow pods and pillow breccia by sulphides, "B" horizon.


CM 1 2 3 4 5 6 7 8 9 10 11 12 13 14 1


CM 1 2 3 4 5 6 7 8 9 10 11 12 13 14 1

PLATE 12. Well-banded sulphides (as indicated) at top of "B" horizon.

PLATE 13. Banding of pyrite and sphalerite (as indicated) near top of "B" horizon. From sample TDH-36a.


Nikon

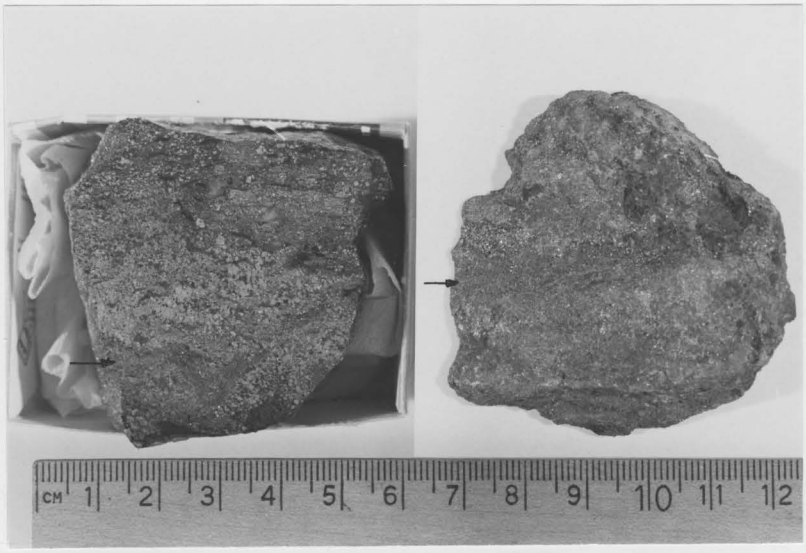
CM 1 2 3 4 5 6 7 8 9 10 11 12

PLATE 14. Fragment textures of sulphides near top of "B" horizon, from sample TDH-36b. Arrows indicate sphalerite, gangue is dark gray to black.


CM 1 2 3 4 5 6 7 8 9 10

predominantly of magnetite with minor pyrite and chalcopyrite in cross-cutting quartz veins. Some malachite is visible in fractures.

Sample locations in the "A" and "B" horizons as well as the local geology are illustrated in figures 3 and 4.

FIGURE 3. Sample locations and local geology of the "A" horizon.

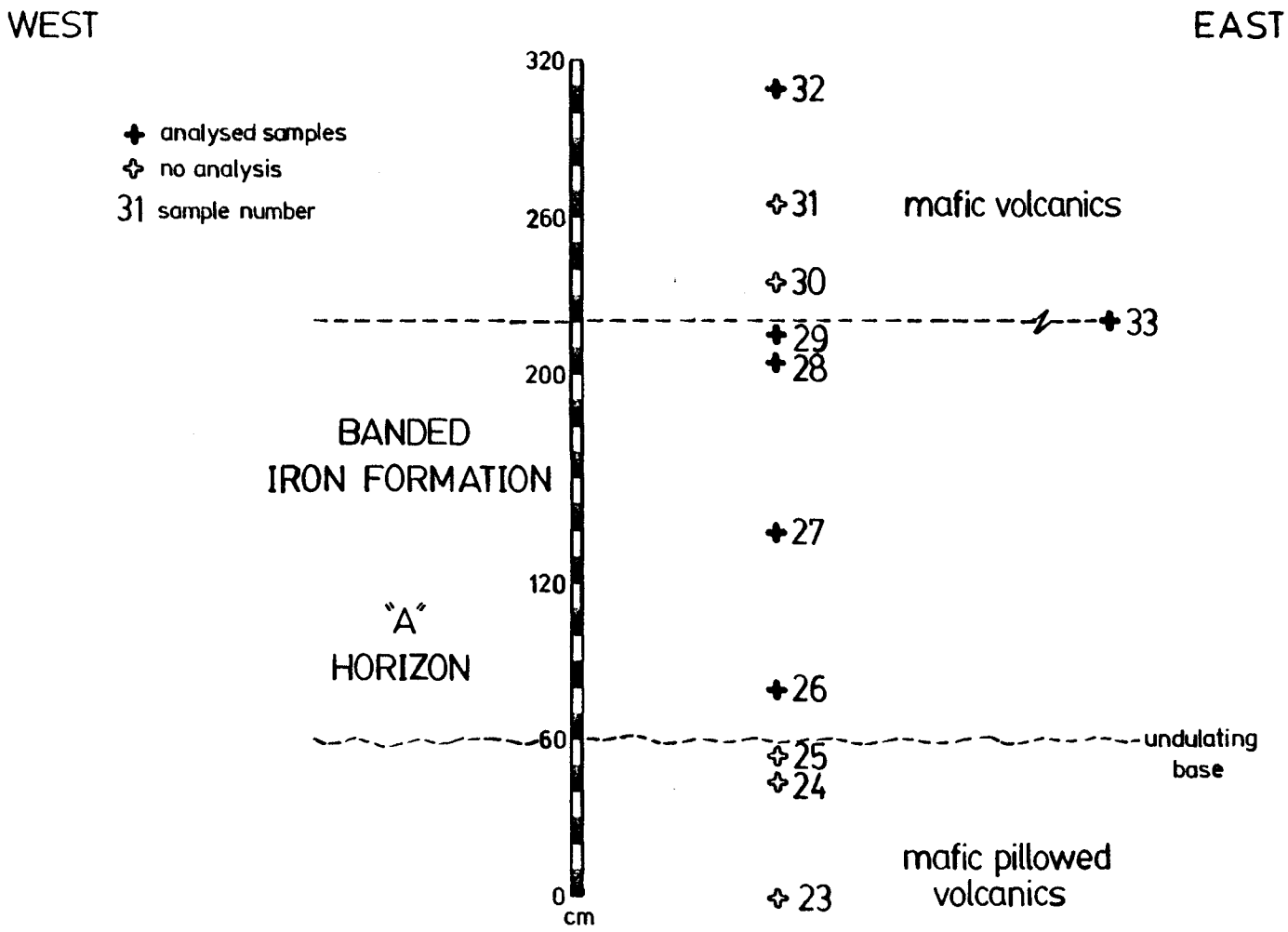
WEST
EAST
analysed samples
no analysis
31 sample number
320
260
200
120
60
0
cm
32
31
30
33
29
28
27
26
25
24
23
mafic volcanics
BANDED
IRON FORMATION
"A"
HORIZON
undulating
base
mafic pillowed
volcanics

FIGURE 4. Sample locations and local geology of the "B" horizon.

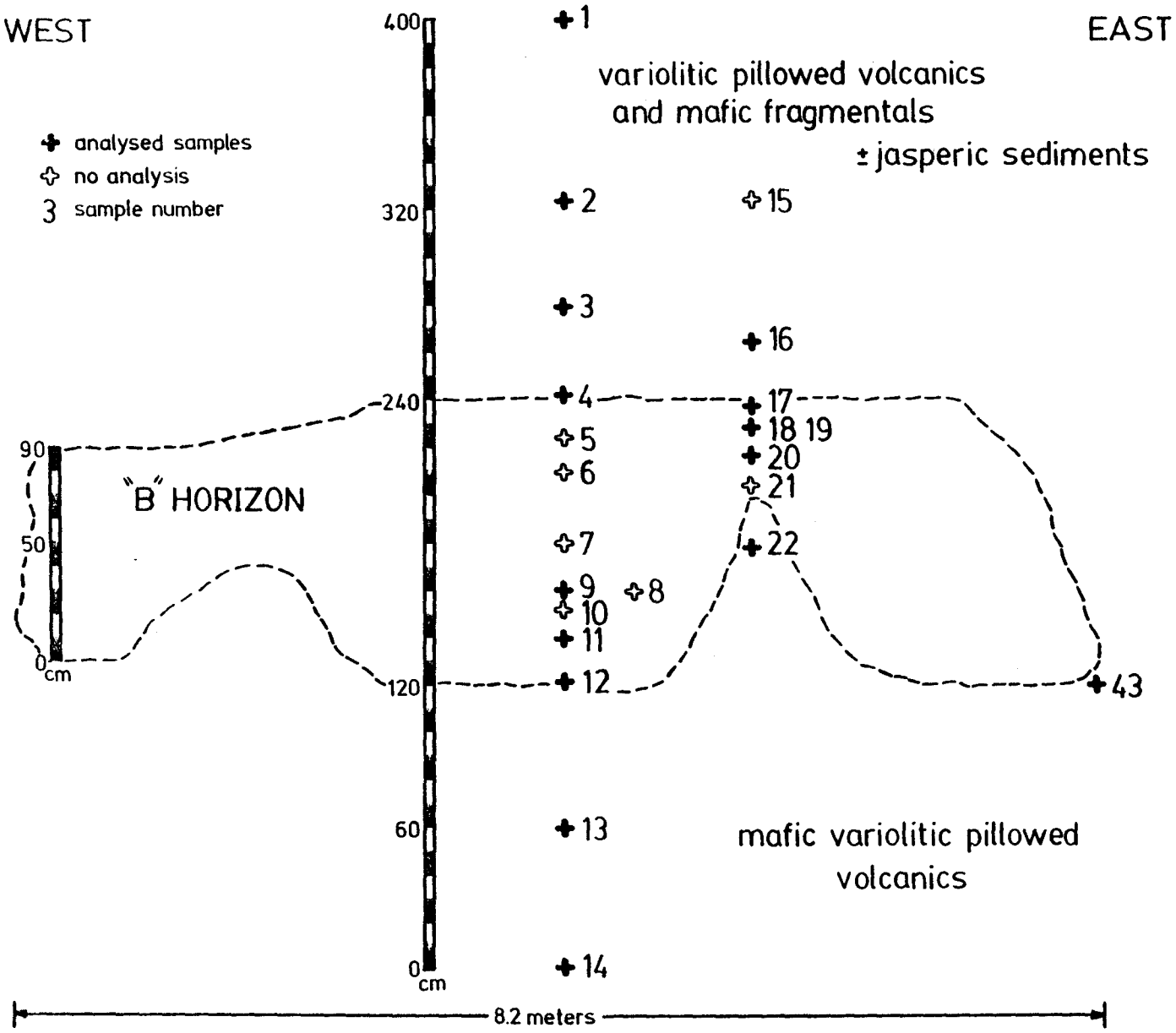
WEST
EAST
analysed samples
no analysis
3 sample number
400
320
240
120
60
0
cm
90
50
0
cm
"B" HORIZON
1
variolitic pillowed volcanics
and mafic fragmentals
± jasperic sediments
2
15
3
16
4
17
18 19
5
20
6
21
7
22
9
8
10
11
12
43
13
mafic variolitic pillowed
volcanics
14
8.2 meters

CHAPTER 3

PETROGRAPHY AND GEOCHEMISTRY

3.1 PETROGRAPHY

The mineralogy of the Tilt Cove Mine and "B" horizon reflect greenschist facies metamorphism.

3.1.1 Tilt Cove Mine

The petrography of the Tilt Cove Mine is best described by Upadhyay (1973). The ore bodies are hosted in heavily chloritized variolitic pillow lava, pillow breccia and agglomerates. Textual features common to the rocks include sedimentary lamination and slump folds.

Upadhyay (1973) describes the mineralogy as consisting primarily of amphibole (>60%), chlorite, plagioclase, clinopyroxene and minor epidote, quartz, calcite and opaques. The amphibole and plagioclase frequently form rosettes. Alteration of clinopyroxene to tremolite-actinolite and eventually chlorite is common. Plagioclase of oligocene-andesine composition is often altered to saussurite. Minor amounts of zoisite, clinozoisite and chromite are occassionally present.

The immediate footwall rocks are fine grained, black and intensely chloritized. This is reflected in their mineralogy (up to 80% chlorite, Kusmirski, 1982 pers. com.). In thin section the footwall rocks are fine- to medium-grained, foliated and locally granulated. The matrix consists predominantly of anhedral quartz mosaics, berlin-blue chlorite and minor

plagioclase. Irregular clusters and rosettes of quartz along with occasional phenocrysts of plagioclase (commonly rimmed by chlorite) are dispersed throughout the matrix. Minor opaques within the sections are often partially altered to biotite.

3.1.2 "B" Horizon

The mineralogy of the "B" horizon host volcanics consists predominantly of berlin-blue chlorite (penninite) and quartz with minor plagioclase, calcite and opaques. The matrix is essentially a felted mass of penninite with interstitial anhedral grains of quartz, plagioclase and calcite. Highly altered plagioclase rosettes exhibit weak relict twinning with angles indicative of low An content. Quartz-calcite veinlets with brown chloritic rims are common. Individual phenocrysts of quartz and calcite are also rimmed by both brown clorite and penninite. In the strongly variolitic sample (TDH-43) the individual varioles were composed of heavily altered quartz ± plagioclase and brown chlorite intergrowths which radiate outwards. Some varioles exhibit almost total replacement by the brown chlorite. The varioles are hosted in a felted mass of penninite. The penninite cuts the varioles locally in small fractures.

A similar mineralogy occurs in the mafic volcanics about the overlying iron formation ("A" horizon). The footwall rocks consist essentially of chlorite (>75%) with appreciable amounts of calcite. Course-grained, sub-rounded calcite crystals are again rimmed by chlorite. It is also common to find discrete chlorite crystals with quartz cores. The matrix consists of an anhedral mass of chlorite, calcite, quartz and plagioclase. Opaques constitute approxiamately three modal percent of the sections. The hanging wall volcanics consist of chlorite with course-grained crystals of calcite and occassionally quartz and plagioclase laths in an anhedral

matrix of calcite, chlorite, plagiocalse and quartz. The plagioclase laths are highly altered through some relict twinning is still evident indicating generally a low An content.

3.2 GEOCHEMISTRY

3.2.1 Tilt Cove Mine

The main pillow volcanics hosting the Tilt Cove ore body have most recently been interpreted as basaltic-komatiitic to magnesium-tholeiitic in composition (Kusmirski and Norman, 1981). Geochemical analysis by Upadhyay (1973), Strong (1980) and Kusmirski (1982 pers. com.) show conflicting trends for CaO and total alkalis. Upadhyay (1973) describes the mafic pillows as enriched in Na_2O and depleted in K_2O. Strong (1980) suggests a depletion of Na_2O and an addition of both CaO and K_2O. Analysis of the host rocks in the 1981 field season (Kusmirski, 1982 pers. com.) show depletion in both alkalis and an Fe:Mg ratio of 2:3. The chloritized footwall rocks were found to be completely void of Na_2O, K_2O and CaO ; depleted in SiO_2 ; and enriched in Fe (up to 30 wt.%).

3.2.2 "B" horizon

The "B" horizon host volcanics were classified using the cation diagram of Jensen (1976) as illustrated in Figure 5. The immediate host rocks plotted exclusively as high-magnesium tholeiites. A sample of mafic volcanic rock form from above the "A" horizon plots at the transition of magnesium tholeiite-balsaltic komatiite. The AFM diagram in Figure 6 is misleading in its classification of the volcanics as being calc-alkaline. The calc-alkaline composition reflects a high secondary Na_2O content from alteration.

The chemical composition of the pillowed volcanics by major element

FIGURE 5. Jensen Cation Plot for classification of "A" and "B" horizon host volcanics.

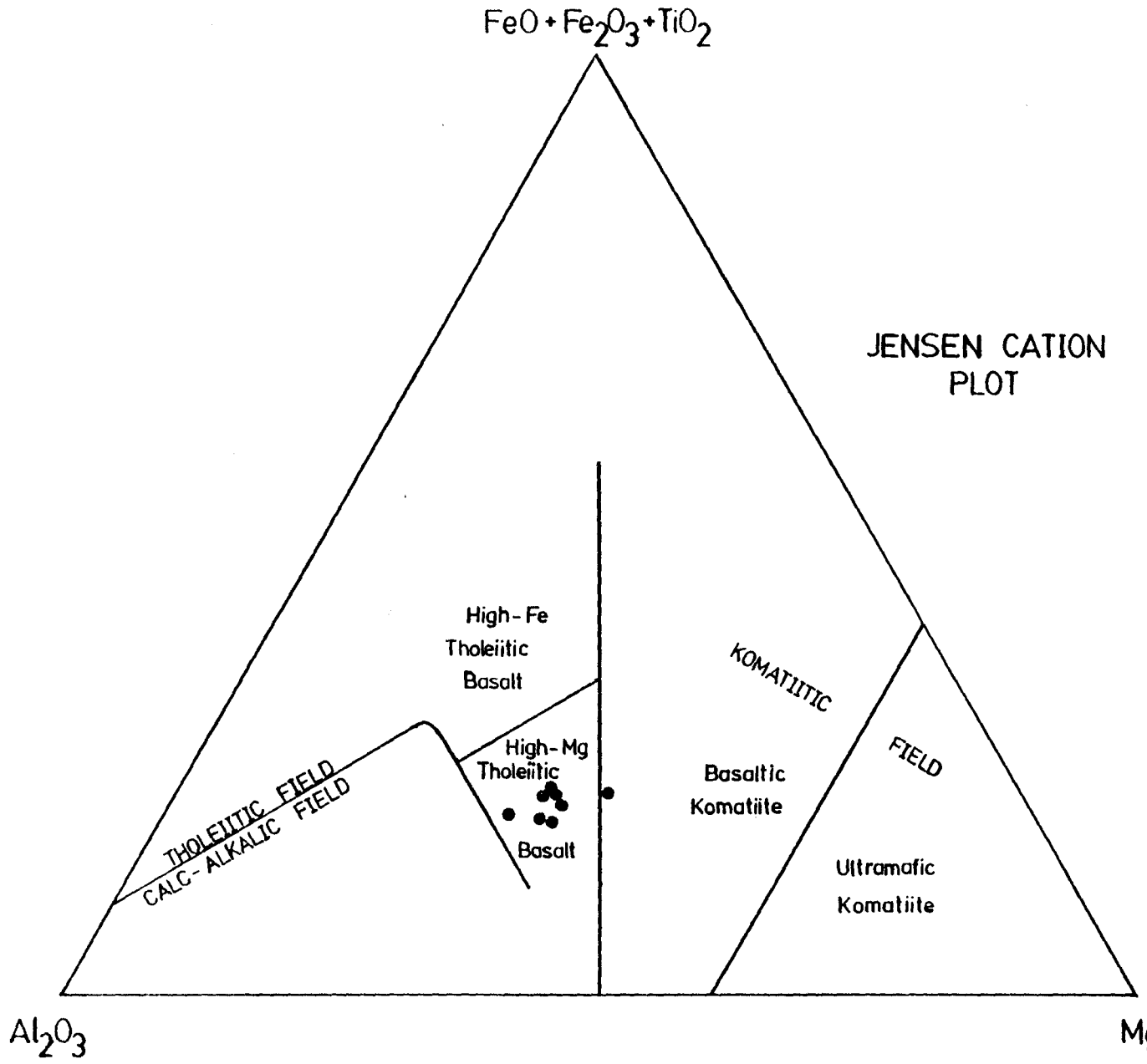
FeO + Fe2O3 + TiO2
JENSEN CATION PLOT
High-Fe Tholeiitic Basalt
High-Mg Tholeiitic Basalt
THOLEIITIC FIELD
CALC-ALKALIC FIELD
KOMATIITIC FIELD
Basaltic Komatiite
Ultramafic Komatiite
Al2O3
MgO

FIGURE 6. AFM diagram for classification of "A" and "B" horizon host volcanics.

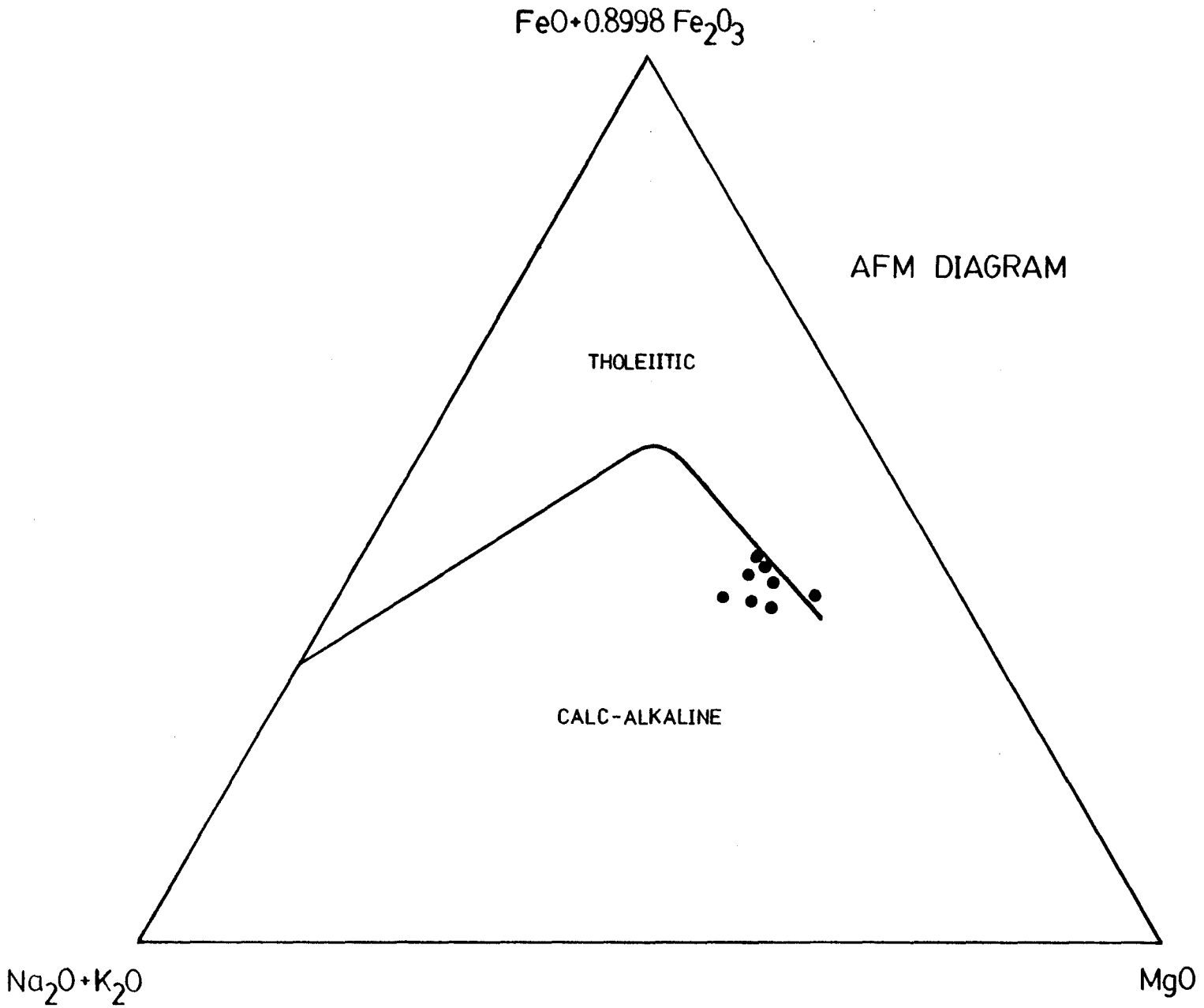
FeO+0.8998 Fe2O3
AFM DIAGRAM
THOLEIITIC
CALC-ALKALINE
Na2O+K2O
MgO

analysis is consistent with that of ocean-floor basalts outlined in Manson (1967) and Stanton (1972). The only noted deviations in chemistry were the weight percent values of Na_2O, CaO and K_2O. In average unaltered ocean-floor basalts the range for Na_2O is approxiamately 2.58 to 3.01 (average 2.85). CaO values from 10.46 to 11.51 (average 11.01) and K_2O values from 0.08 to 0.21 (average 0.16 ; Stanton, 1972). The range of Na_2O in the "B" horizon host volcanics is 4.40 to 5.17 (average 4.71) weight percent. Spilitization of the rocks would account for the substantial increase from the norm. CaO values are relatively low with a range of 0.74 to 6.69 (average 2.63) weight. K_2O has been depleted to less than the detection limit of 0.20 weight percent. Both CaO and K_2O have been lost during chloritization of the rocks.

Most trace element values for the host volcanics are consistant with the average values for ocean ridge basalts, outlined by Kay and Hubbard (1978). Cr values however, are somewhat higher than the recorded range of 35 to 510 (avergae 247) ppm. In the "B" horizon host rocks the range in Cr content is 415 to 685 (average 544) ppm. Fe:Mg ratios for the host volcanics are approxiamately 1.1:1, however, this is not a true ratio as some secondary Fe enrichment has taken place during chloritization.

Weight percent of volatiles in the host rocks ranges from 4.00 to 5.94. A value of 7.96 wt % was attained from the volcanics above the "A" horizon. No correlation is apparent between gold and degree of alteration (L.O.I.) in the volcanics. A completely random pattern is evident (Table C-1, C-2).

Figure 7 displays the relative amounts of Au, As and Sb in the hanging wall and footwall rocks to the ore zone. A positive correlation is evident in the rocks of the hanging wall in that as Au values increase and decrease, so do values for As and Sb. This positive correlation is

FIGURE 7. Profile of Au, As and Sb in the hanging wall and footwall rocks to the "B" horizon. Samples 16, 22 and 43 lie outside of the vertical section (Figure 4) and hence are not joined by lines.

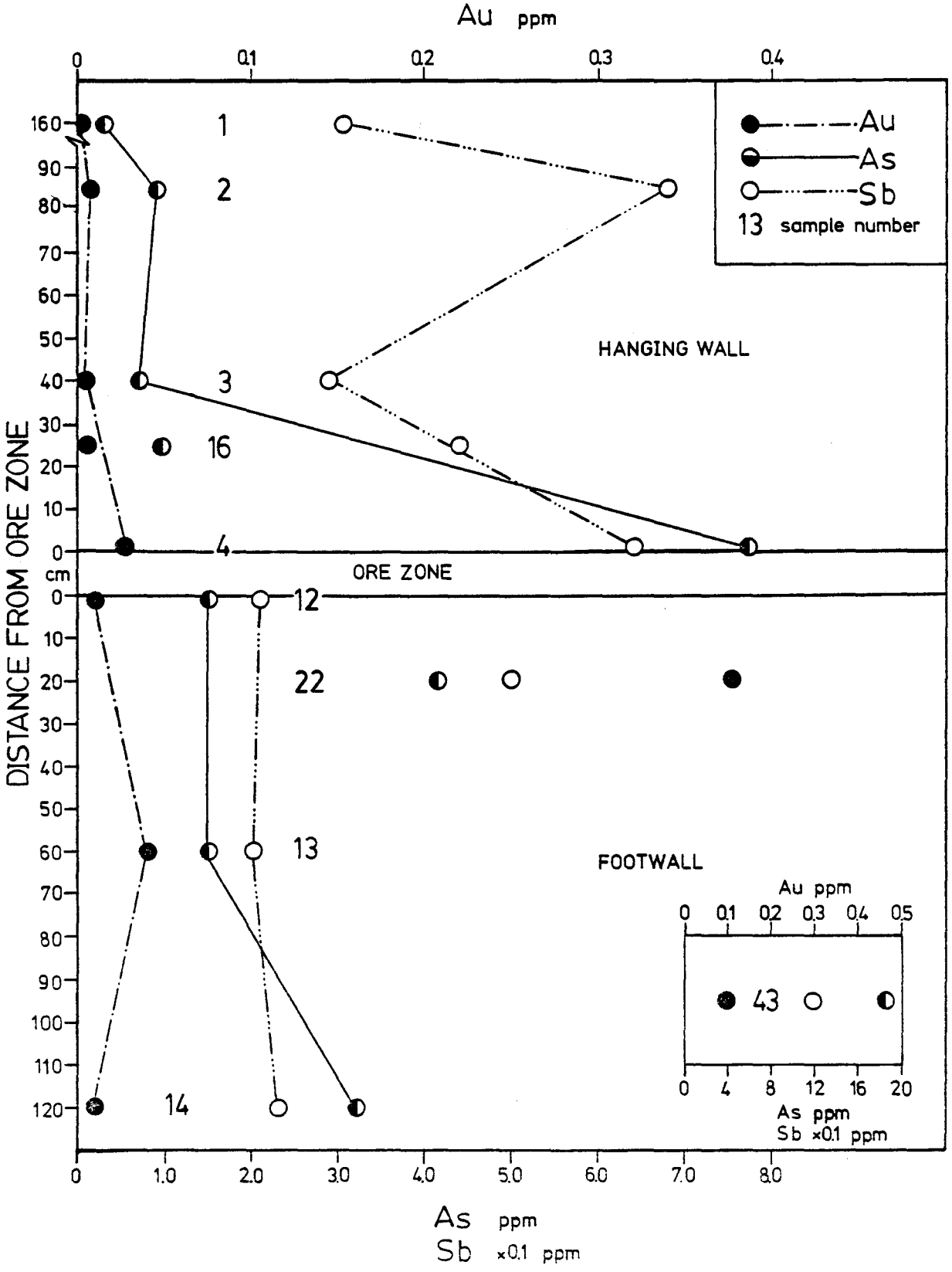
Au ppm
0
0.1
0.2
0.3
0.4
Au
As
Sb
13 sample number
HANGING WALL
ORE ZONE
FOOTWALL
DISTANCE FROM ORE ZONE
cm
160
90
80
70
60
50
40
30
20
10
0
1
2
3
16
4
12
22
13
14
43
Au ppm
0 0.1 0.2 0.3 0.4 0.5
0 4 8 12 16 20
As ppm
Sb ×0.1 ppm
0 1.0 2.0 3.0 4.0 5.0 6.0 7.0 8.0
As ppm
Sb ×0.1 ppm

not seen in footwall rocks although it is noteworthy that generally where Au values are low As and Sb values are also low, and where Au value is high (TDH-22), As and Sb values are also high. Unfortunately this trend is not seen in the strongly variolitic volcanics (TDH-43 insert) where a low Au value is accompanied by very high As and Sb values. The profile also shows that though gold values are higher in adjacent samples they exhibit no systematic gradient away from the ore zone.

Figure 8 illustrates the relationships between Au, As and Sb within the ore zone. Values for all three elements are significantly higher than in the enclosing volcanics. The three samples exhibiting high values in gold (>28 ppm) are sphalerite enriched. No correlation for Au, As and Sb is apparent below a threshold of 4 ppm Au. Above this threshold a negative correlation exists and may be due to an association of gold with sphalerite.

A plot of Au versus Cu, Zn and S for the "B" horizon samples is illustrated in Figure 9. There is no correlation between Cu, S and Au. Au versus S produces a scattered array, and Au versus Cu a vertical line. Whether a correlation exists between Au and Zn is uncertain. A correlation coefficient would only give a biased value due to the high Zn / high Au sample. Intermediate analysis between this sample and the low Zn / low Au samples is needed to make any conclusions over the relationship.

Mineral separates of samples from the "B" horizon, the fault zone (above the "B" horizon) and the East Mine, were analysed for As, Sb and Au. Samples 37a and 37b (Table C-6) are chalcopyrite and hematite separates from the fault zone. Both exhibited low Au values of 0.08 ppm and 0.04 ppm respectively. Sample TDH-40a is a chalcopyrite separate of TDH-40, a relatively pyrite-rich sample from the East Mine. Its Au value of 0.79 ppm is significantly lower than 1.30 ppm whole rock value of TDH-40. This

FIGURE 8. Au vs. As and Sb in the "B" horizon ore zone.

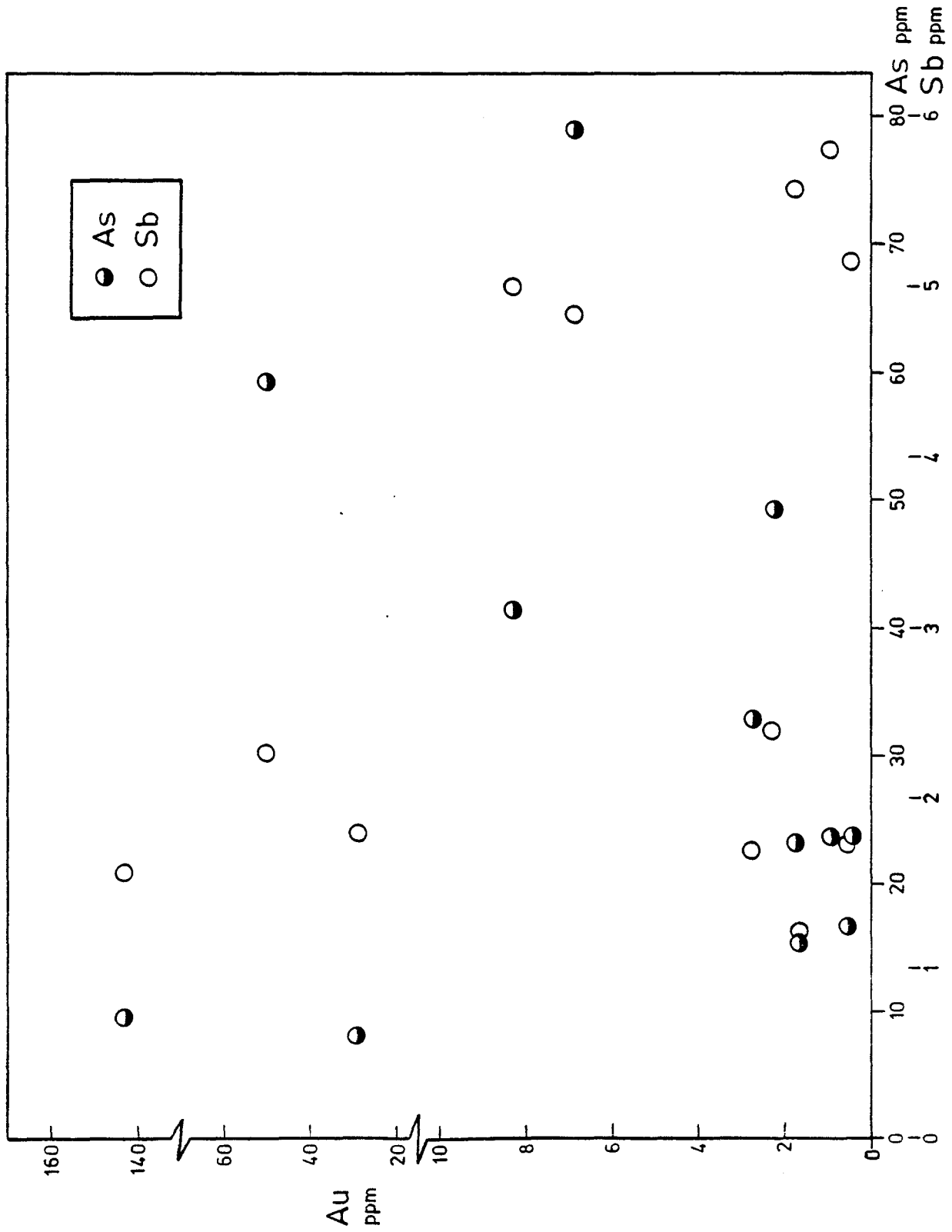
As
Sb
Au ppm
As ppm
Sb ppm
160
140
60
40
20
10
8
6
4
2
0
80
70
60
50
40
30
20
10
0
6
5
4
3
2
1
0

FIGURE 9. Au vs. Cu, Zn and S in the "B" horizon ore zone.

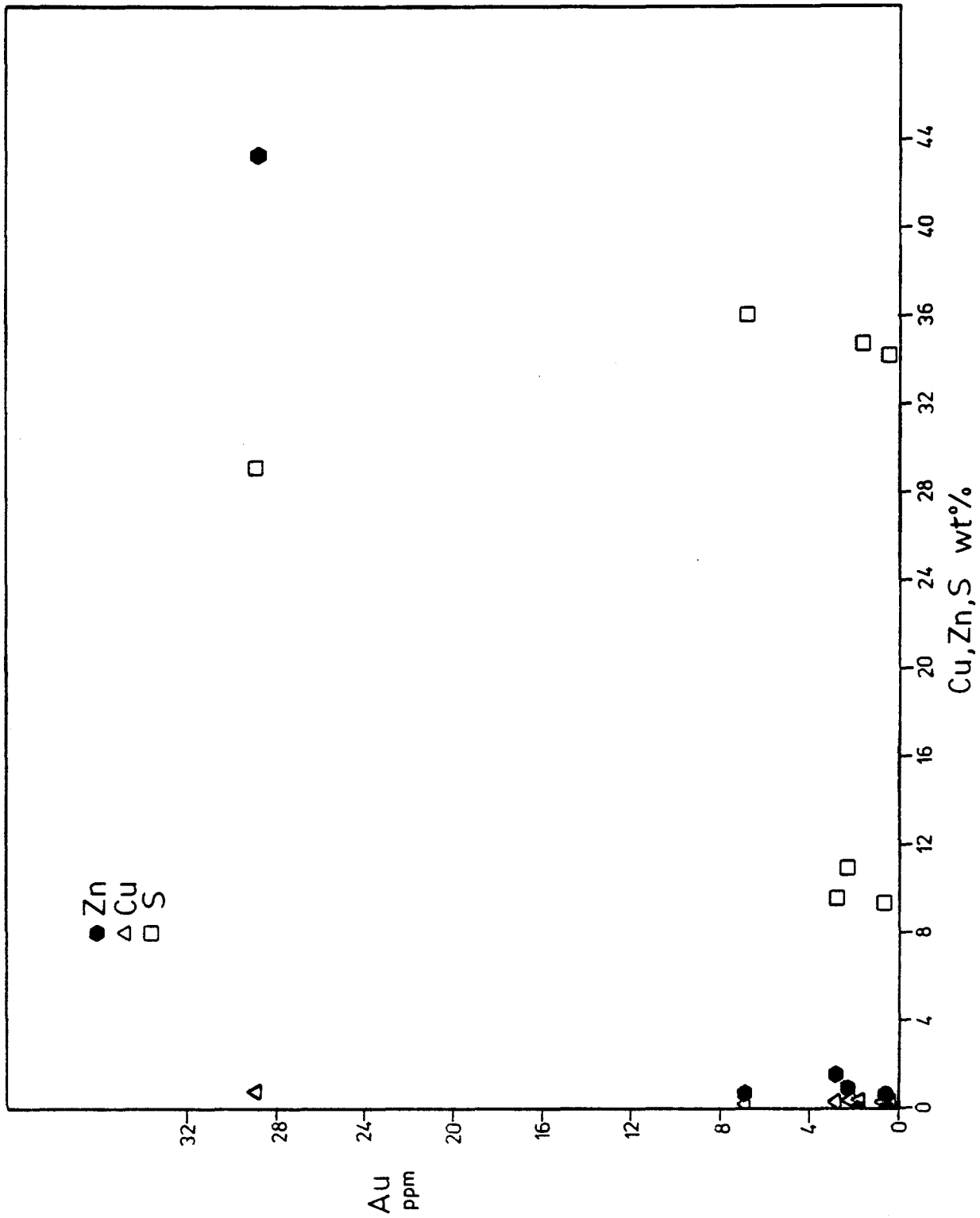
Zn
Cu
S
Au
ppm
Cu,Zn,S wt%
0
4
8
12
16
20
24
28
32
36
40
44

implies that gold is not selectively concentrated by (or in) chalcopyrite in the East Mine. Sample TDH-19a is a sphalerite separate of TDH-19 from the "B" horizon. It has a gold content of 140 ppm which is significantly higher than the 29 ppm value of TDH-19, implying a strong relationship between Au and sphalerite. TDH-19 itself is sphalerite-rich and exhibits the highest Au value of the "B" horizon sulphide samples. The Au-sphalerite relationship is again implied in the separates of TDH-18 from the "B" horizon. TDH-18a and TDH-18b are pyrite + silicate and pyrite +sphalerite separates respectively. The Au values for the two separates are 1.7 ppm and 50 ppm. If the Au was associated with pyrite, higher values would be expected. It seems more likely that the Au is strongly associated with sphalerite.

CHAPTER 4

METALLOGRAPHY AND ORE TEXTURES

4.1 TILT COVE MINE

The ore body at Tilt Cove Mine is best described by Upadhyay (1973), who characterized the ore as massive fine-grained steeply dipping pyrite bodies with chalcopyrite, and diffused stockworks of stringers, veins and irregular clusters of pyrite and chalcopyrite. The chief metallic minerals of the mine are pyrite (py), chalcopyrite (cpy), minor magnetite (mte), sphalerite (sph) and native gold and silver. Specularite and limonite occur in the vicinity of strong post-ore slips within massive sulphide zones. Upadhyay suggested the following paragenesis :- mte → py → po → cpy → sph with cpy replacing nearly all earlier minerals. The following observations were made by the author on several polished sections from the East Mine. The dominant metallic minerals in the sections are pyrite, magnetite and hematite (hem), followed by chalcopyrite, sphalerite and minor covellite (cov).

Magnetite occurs as euhedral grains (Plate 15) and irregular masses. Many of the small idiomorphic crystals contain a minute euhedral inclusion (Plate 15). The inclusions are metallic, and darker in colour. Attempts at microhardness testing resulted in complete destruction of the crystals. Hematite is present as distinct blades and radiating acicular crystals (Plates 16 and 18). Some hematite blades are seen to skewer others. The hematite commonly surrounds and includes the larger euhedral magnetite

PLATE 15. Magnetite rhombs with unidentified inclusions, from sample TDH-35, East Mine. Field of view is 1.1 mm.

PLATE 16. Radiating accicular crystals of hematite, from sample TDH-42, East Mine. Field of view is 2 mm.

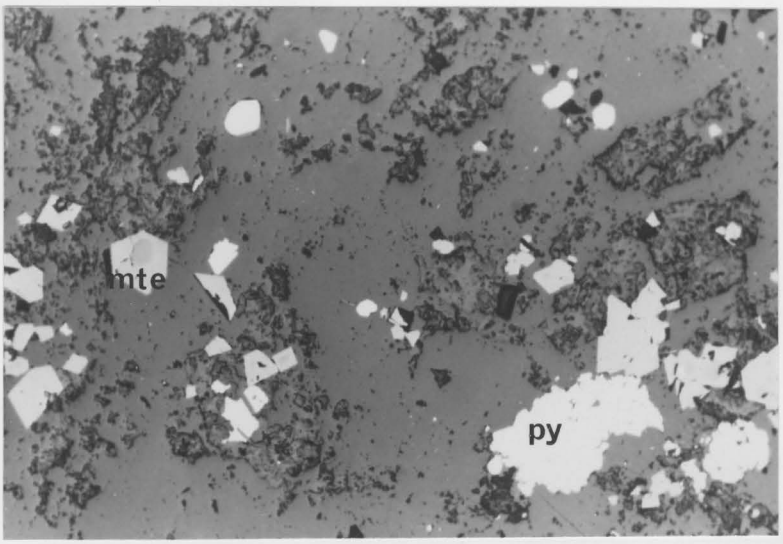
mte
py

PLATE 17. Colloform banding of pyrite (py) and chalcopyrite (gray), from sample TDH-40 East Mine. Field of view is 2 mm.

PLATE 18. Colloform pyrite (py) and hematite blades, from sample TDH-41, East Mine. Field of view is 2 mm.

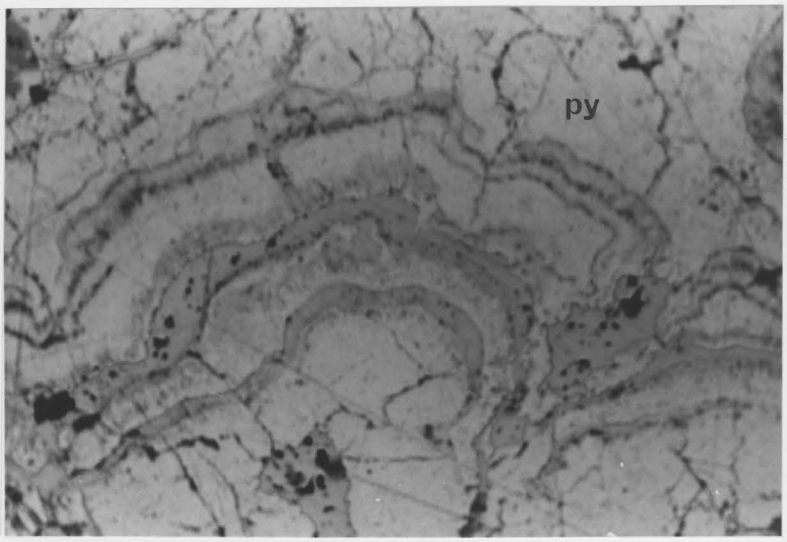
py

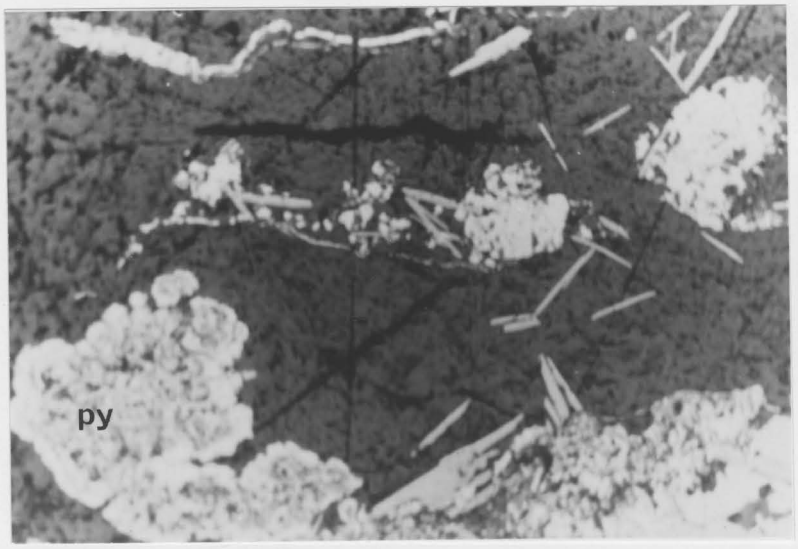
py

grains and masses. In some sections it appears to be replacing the magnetite. Other sections show acicular and radiating hematite growing outwards from magnetite into silicate gangue.

Several sections show prominent colloform texture with alternating bands of pyrite and chalcopyrite, (Plates 17 and 18). The texture represents chemical co-precipitation of the two minerals. Distinct spheroids of pyrite closely resembling framboids are dispersed throughout the colloform bodies. They range in size from 10 to 50 μm with some of the larger spheroids exhibiting possible overgrowths. Though much of the internal structure has been lost some framboids reveal a microcrystalline core. Intermediate textures between the spherical framboids and euhedral pyrite crystals of the colloform bodies are common. As with the colloform texture, framboidal pyrite is formed by chemical precipitation of either a colloidal or supersaturated solution (Chen, 1978). Large veins of chalcopyrite are seen to disrupt and crosscut the colloform bodies. The chalcopyrite is either secondary or remobilized. Due to the relatively unaltered nature of the framboids within the chalcopyrite it seems more likely that the mineral is only remobilized. In other sections pyrite occurs as euhedral to subhedral grains often showing partial replacement of magnetite and hematite. Chalcopyrite in turn replaces pyrite as well as the oxide minerals.

Sphalerite appears relatively late in the paragenesis replacing pyrite, chalcopyrite and filling fractures in the colloform pyrite. Minor covellite is seen replacing rims of chalcopyrite and sphalerite.

A suggested paragenesis for the non-colloform East Mine sections is: -

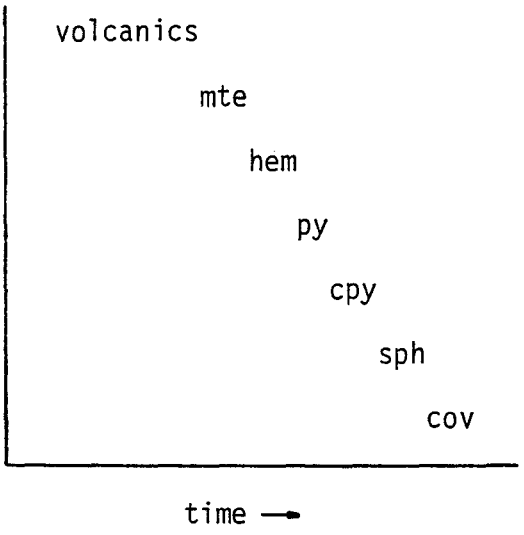

In the colloform sections, chalcopyrite is crystallized intermittantly with pyrite. No covellite was present in these sections. The suggested paragenesis is: -

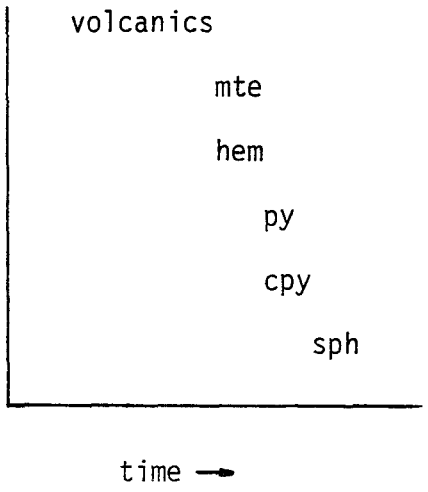

Note: Magnetite or hematite occur in these sections. The two oxides do not occur together.

4.2 "B" HORIZON

Polished sections from the "B" horizon host a wide variety of textures and interesting mineral relationships. The disseminated to massive ores contain from 35 to 95 percent sulphides per section. Pyrite is the dominant metallic mineral followed by chalcopyrite, sphalerite, minor covellite, hematite and native gold (Au).

Volcanics hosting the mineralization in the "B" horizon are occasionally fragmental in character. In polished section the sulphides surround fragments and occur as minor dissemination within them (Plate 19). The surrounding of micro-fragments produces an interesting coronal texture (Plates 20 and 24).

Banding of pyrite (Plate 21), and pyrite with sphalerite (Plate 22) is consistant with the stratiform nature of the ore deposit. The presence of sphalerite in bands results from direct replacement of the original pyrite layer. Remnants of replaced pyrite are common in the sphalerite.

Pyrite exhibits a variety of textures produced by mild deformation and strain. Large idioblastic crystals of pyrite in close proximity to smaller anhedral grains suggests possible recrystallization. The anhedral grains may also result from growth impingement during replacement of the silicate material. The pyrite also exhibits possible subgraining in some samples when viewed under crossed nicols. Stanton (1972) does not acknowledge the possibility of subgraining in pyrite. Perhaps the optical property developed during polishing. Overgrowths of pyrite often enclose aggregates of inclusions and primary fractured pyrite. Occassionally an arc of inclusions is present representing the former crystal boundary. Through a relatively minor phase, brittle deformation is evident in the form of cataclastic pyrite (Plate 23).

PLATE 19. Disseminated sulphides in fragmental volcanics, from sample TDH-9, "B" horizon. Field of view is 2.3 cm.

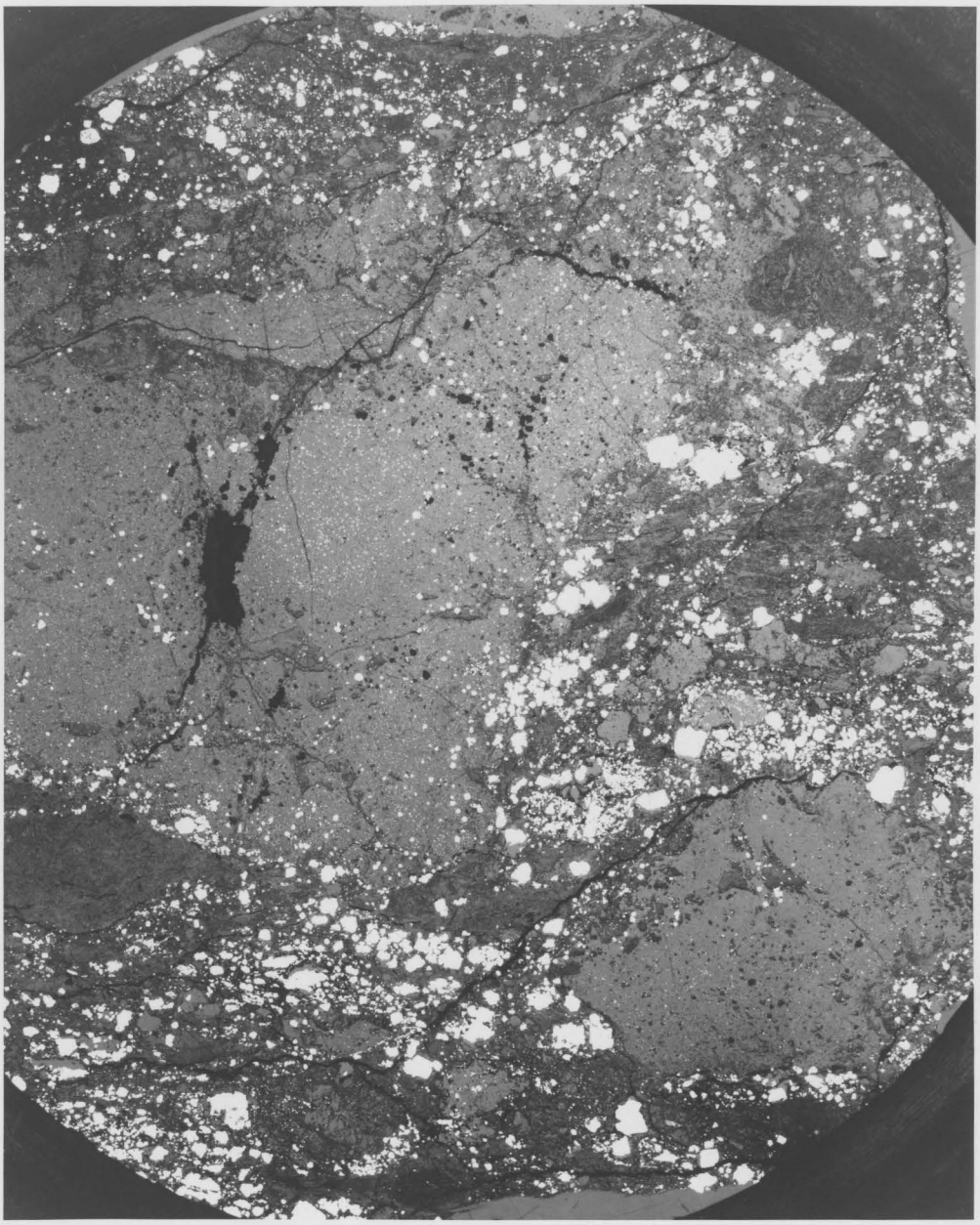

PLATE 20. Microfragments surrounded by sulphides - coronal texture, from sample TDH-44e, "B" horizon. Field of view is 2 mm.

PLATE 21. Banding of pyrite, possible recrystallization, from sample TDH-20, "B" horizon. Field of view is 2 mm.

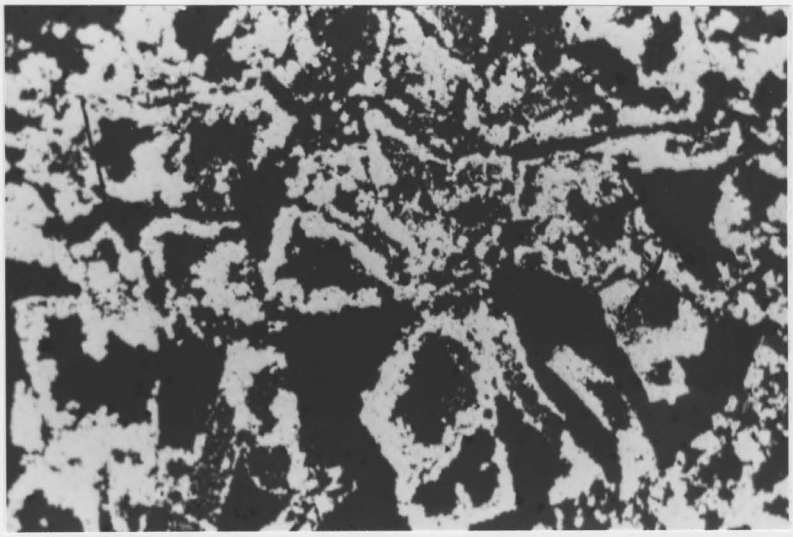

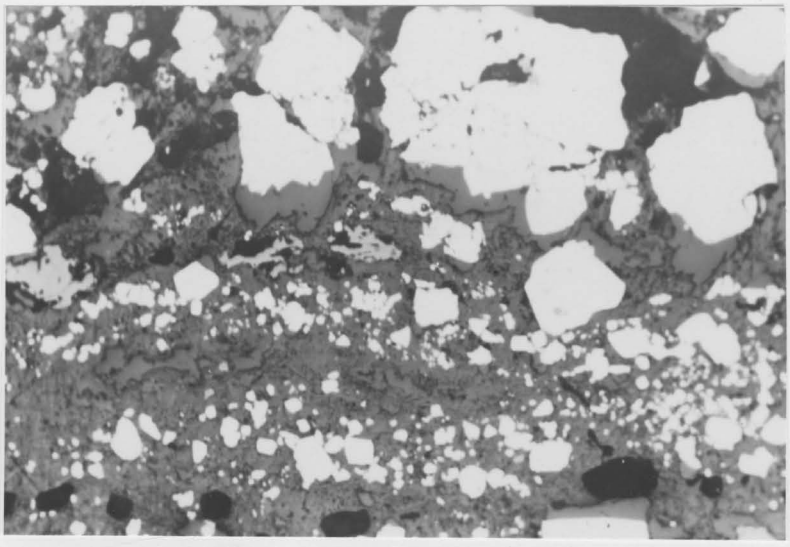

PLATE 22. Banding of pyrite and sphalerite (dark gray) gangue is black. From sample TDH-36a, "B" horizon. Field of view is 2.4 cm.

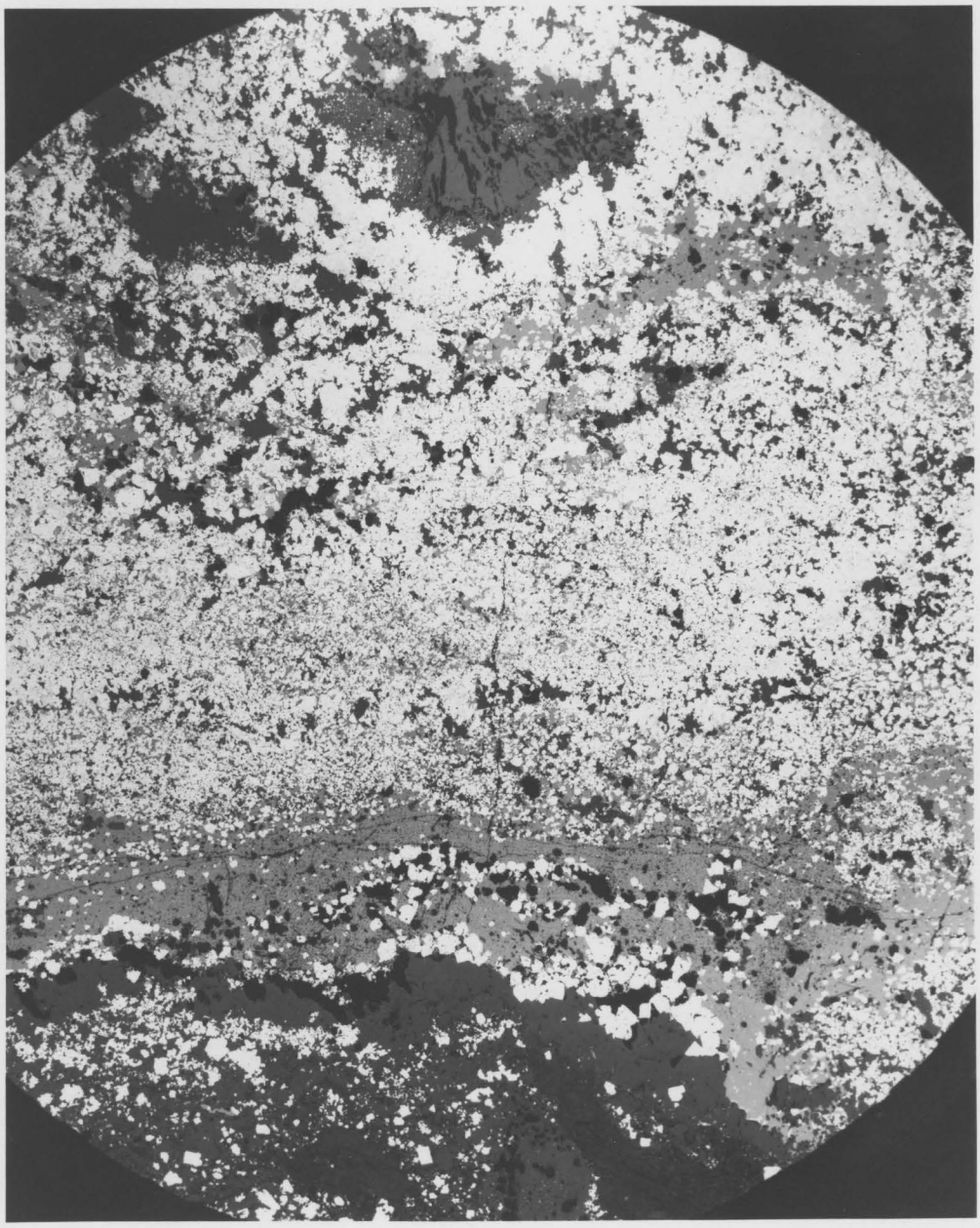

Relict colloform texture involving the banding of pyrite ± chalcopyrite is also present in the "B" horizon ores (Plate 24). The colloform texture as previously mentioned results from chemical precipitation of the sulphides (Chen, 1978). The pyrite-chalcopyrite banding however is not the only evidence for co-precipitation. In Plate 25 the two sulphides form a network surrounding silicate fragments. A close-up of this texture (Plate 26) reveals a spheroidal nature of the pyrite closely resembling the framboids present in the colloform East Mine sample. Sizes of the framboids range from 10 to 150 μm. The average diameter is 50 μm suggesting that the larger grains may have undergone some overgrowth. Embayment of the pyrite by chalcopyrite is very minimal indicating a co-precipitaion of the two sulphides rather than a later introduction of the chalcopyrite.

Many of the sections show a distinct "atoll" texture (Plates 27, 33, 39). Pyrite grains in a matrix of sphalerite commonly host inclusions of sphalerite, chalropyrite and occassionally gold. Pyrite crystals lacking the inclusions are often deeply embayed. The texture results from replacement of the pyrite by each of the minerals. The gold was either released from the pyrite during replacement or was introduced in solution along with the other sulphides. The inclusions tend to amalgamate and migrate toward grain boundaries for eventual expulsion from the pyrite. Pyrite crystals which either have succeeded in expelling the inclusions or were originally replaced at grain boundaries exhibit deep embayments due to loss of volume. In other sections pyrite contains inclusions of chalcopyrite and silicate material representing the replacement of pyrite during alteration of the volcanic host.

Further evidence of replacement of pyrite is pictured in Plate 28.

PLATE 23. Cataclastic pyrite, from sample TDH-17, "B" horizon. Field of view is .55 mm.

PLATE 24. Relict colloform pyrite and surrounding of fragments, from sample TDH-44f, "B" horizon. Field of view is 2 mm.

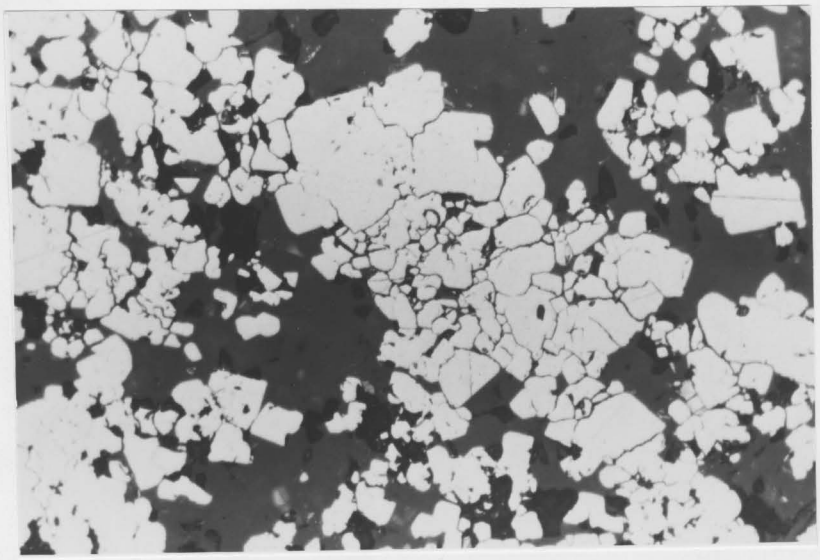

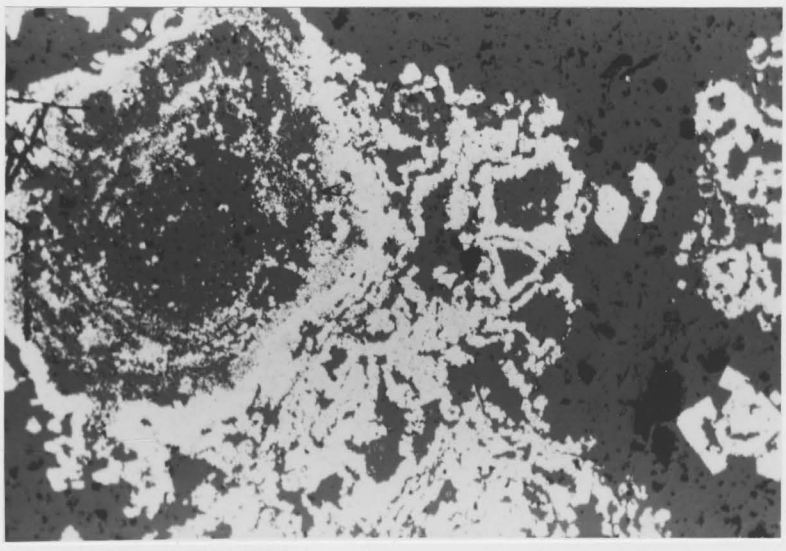

PLATE 25. Network of pyrite and chalcopyrite surrounding fragments. Pyrite is rounded and exhibits higher relief. From sample TDH-11, "B" horizon. Field of view is 2 mm.

PLATE 26. Framboidal pyrite (py) in chalcopyrite (cpy), enlargement of Plate 25. From sample TDH-11, "B" horizon. Field of view is 1.1 mm.

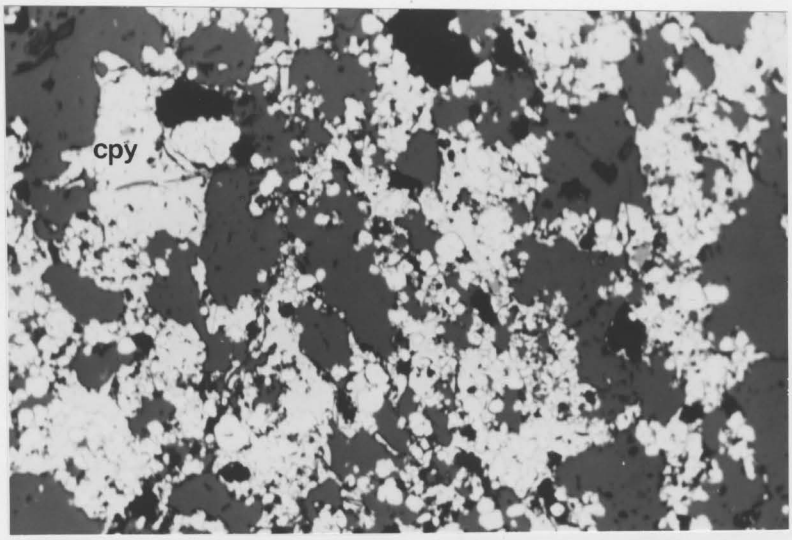
cpy

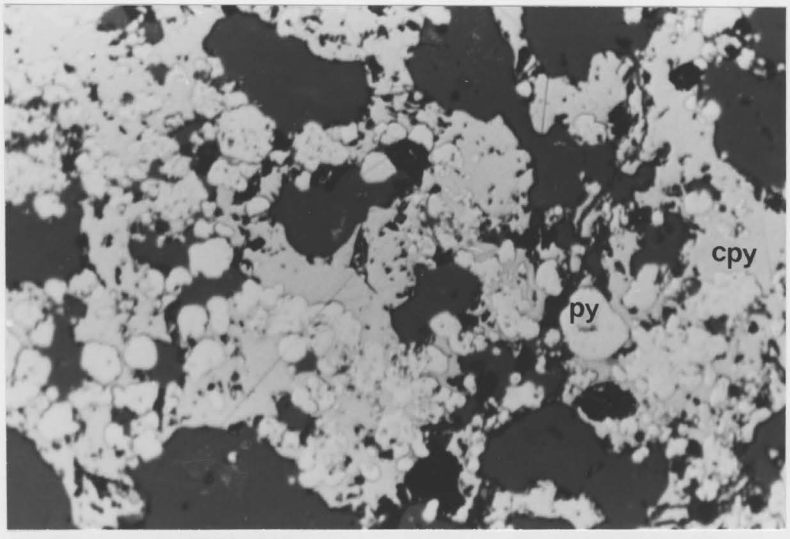
cpy
py

PLATE 27. Pyrite (white) exhibiting distinct atoll textures in a matrix of sphalerite (light gray). From sample TDH- 18, "B" horizon. Field of view is 1.1 mm.

PLATE 28. Replacement of pyrite (py) by chalcopyrite (light gray) and sphalerite (dark gray), gangue is black. From sample TDH-36b, "B" horizon. Field of view is 2 mm.

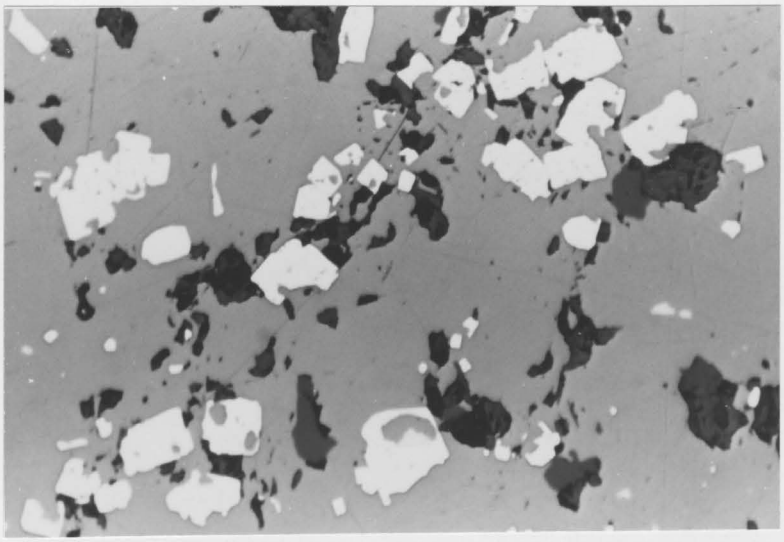

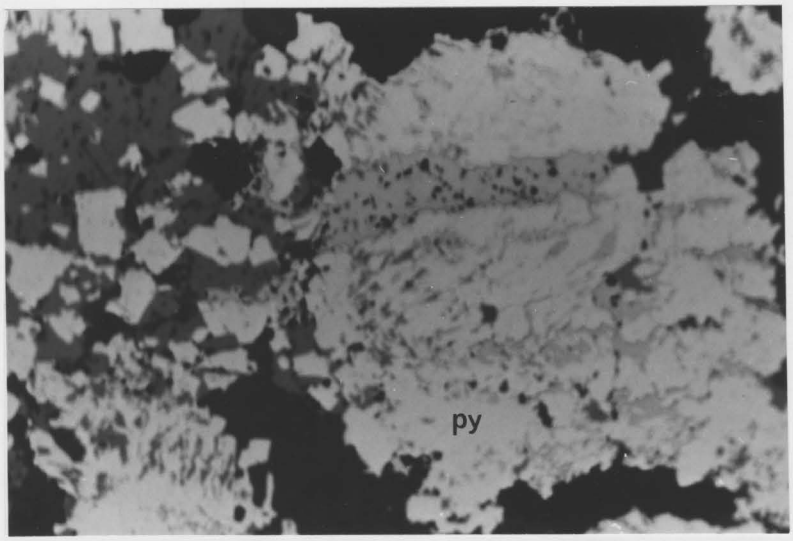
py

Flames and shreds of chalcopyrite and sphalerite are seen to transverse across pyrite grains. The shreds are commonly orientated in three to four directions representing crystallographic directions in the pyrite. Dispersed flames completely enclosed by pyrite resemble exsolution intergrowths. Stanton (1972) does not acknowledge the possibility of pyrite hosting any exsolution bodies nor the possibility of one sulphide exsolving two others. Within the same sample there are occurrences of larger elongated inclusions of chalcopyrite and sphalerite which are oriented parallel to the four sides of the host pyrite cube. Their deviation in appearance from the replacement grains suggests a different mode of origin. The texture possibly formed by co-precipitation of the three minerals where during the successive growth of pyrite, the chalcopyrite and sphalerite were incorporated into the grain along regular crystal faces.

Exsolution intergrowths of chalcopyrite in sphalerite are quite common. The chalcopyrite occurs as a myriad of minute blebs dispersed randomly throughout the sphalerite grain (Plate 41). Exsolution results from the unmixing of a chalcopyrite-sphalerite solid solution during cooling (Stanton, 1972) and thus provides excellent evidence of simultaneous deposition.

Mild deformation of the sulphides is also apparent within the massive sphalerite samples where the sphalerite commonly exhibits lamellar twinning. The twinning probably occurs during annealing where stresses and accumulated strains within the crystal are reduced or eliminated (Stanton 1972). Twin sets are randomly oriented throughout the sphalerite revealing the polycrystalline nature of the otherwise massive-looking mineral.

Covellite occurs in trace amounts throughout most of the sections replacing chalcopyrite, sphalerite and gangue. In Plate 41 the covellite

exhibits replacement of chalcopyrite and gangue along perimeters of grains. Plate 33 illustrates both rim replacement and irregular internal replacement of the gangue. The covellite has only replaced gangue which is in direct contact with sphalerite. No replacement along gangue-pyrite boundaries is visible. Considering that the silicate material predated the pyrite, introduction of the covellite must have occurred contemporaneously with or shortly after replacement of the pyrite and gangue by sphalerite.

Hematite is abundant in one section; however, its radiating and acicular habit around an Fe-Al silicate mineral suggest an alteration origin rather than a hydrothermal fluid source.

Native gold was observed in all but one of the polished sections from the "B" horizon. The section which lacked gold contained over 80 modal percent pyrite. The gold was distinguished from chalcopyrite by its brilliant yellow colour, high reflectivity and brightly speckled, greenish internal reflections. Plate 29 is a microphotograph showing pyrite, chalcopyrite and gold under partially crossed polars. The red tint to the minerals results from the inability of the photographic microscope to have fully crossed polars. The pale pyrite matrix and darker chalcopyrite grains exhibit no reflectance. The gold in contrast is highly reflective internally with a distinctive sparkling surface.

The morphology of gold in some sections closely resembles that of the chalcopyrite which replaces pyrite (Plates 30 and 31). Other morphologies include small anhedral grains (Plates 32, 39 and 41), minute cubes in pyrite (Plates 35 and 36) and irregular clusters (Plates 37 and 38).

Plate 39 shows two grains of gold completely enclosed within a pyrite crystal. The gold was probably introduced during the replacement of pyrite by chalcopyrite and sphalerite. One grain of gold appears to embay

PLATE 29. Bright internal reflectance of gold (Au), partially crossed polars. From sample TDH-38, "B" horizon. Field of view is 180 μm.

PLATE 30. Gold (Au) in pyrite, from sample TDH-38, "B" horizon. Field of view is 180 μm.

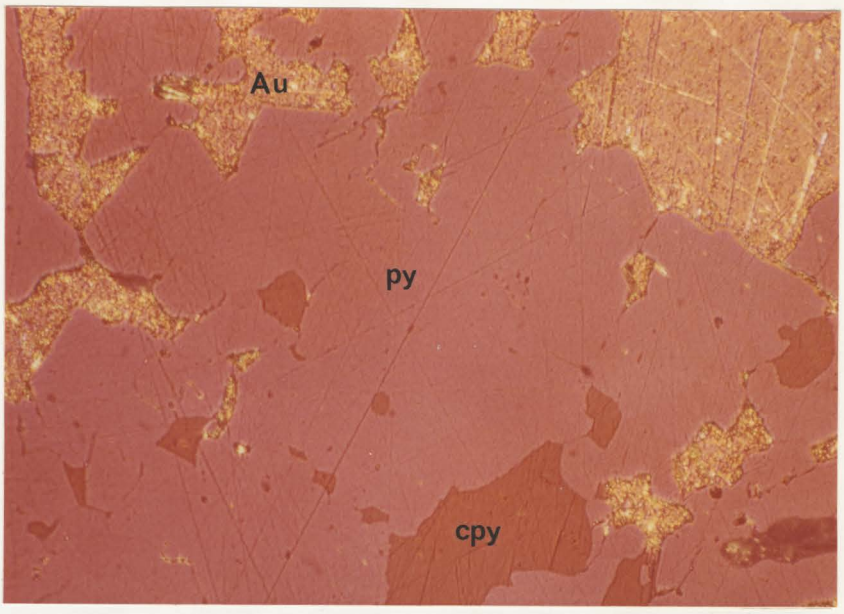
Au
py
cpy

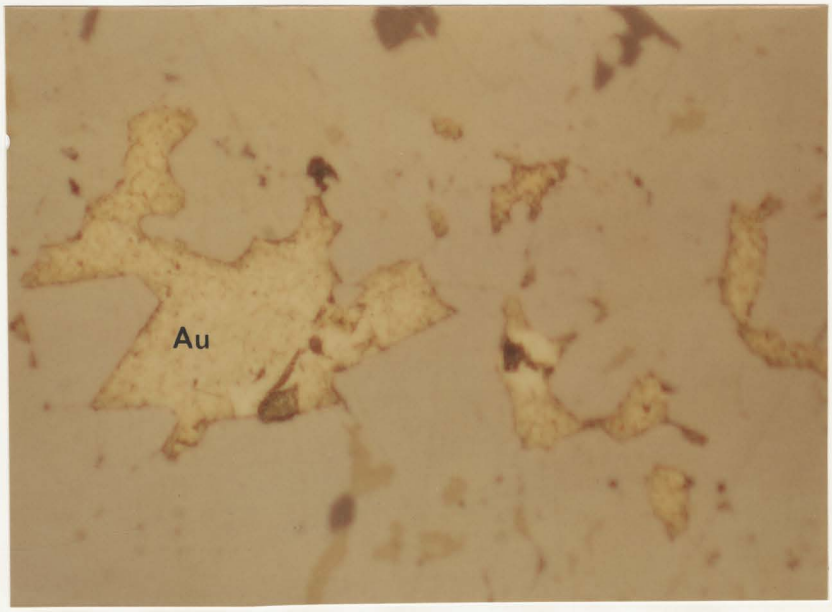
Au

PLATE 31. Gold (Au) and chalcopyrite (cpy) in pyrite (py). From sample TDH-38, "B" horizon. Field of view is 180 μm.

PLATE 32. Gold (Au) and pyrite (py) in sphalerite (light gray). From sample TDH-38, "B" horizon. Field of view is 180 μm.

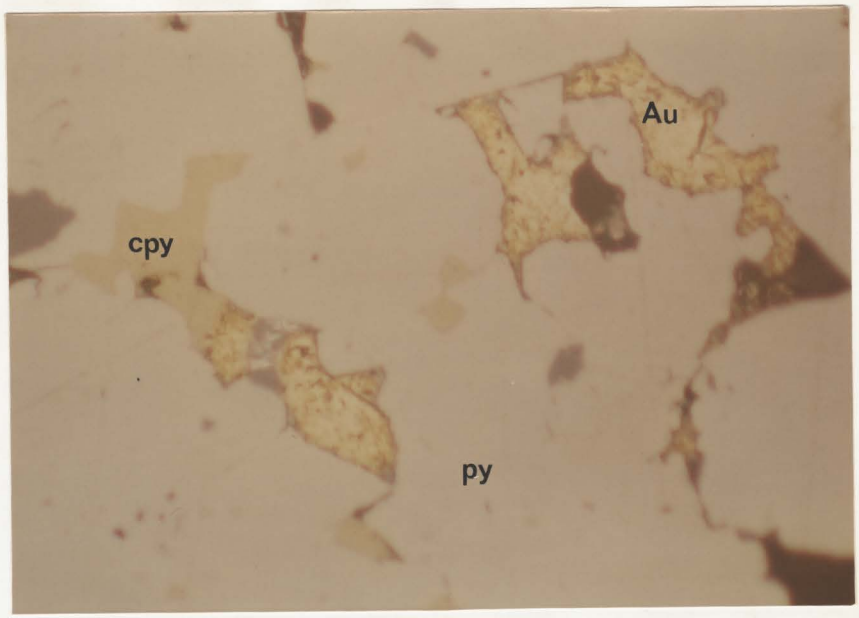
Au
cpy
py

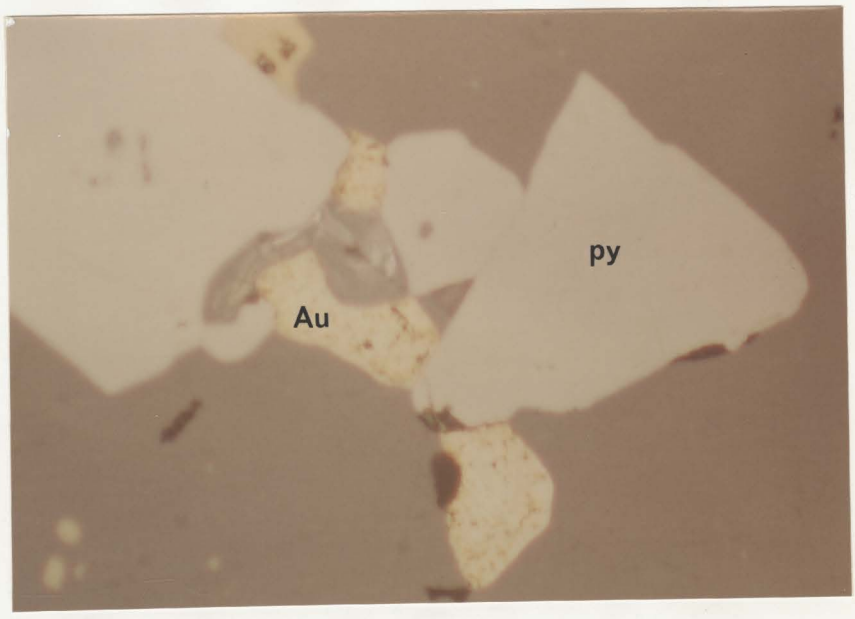
py
Au

PLATE 33. Gold (as indicated) in pyrite. Pyrite exhibits atoll texture, covellite (blue) is replacing gangue. From sample TDH-18, "B" horizon. Field of view is .5 mm.

PLATE 34. Large flake of gold (Au) in gangue (black), from sample TDH-36b, "B" horizon. Field of view is .5 mm.

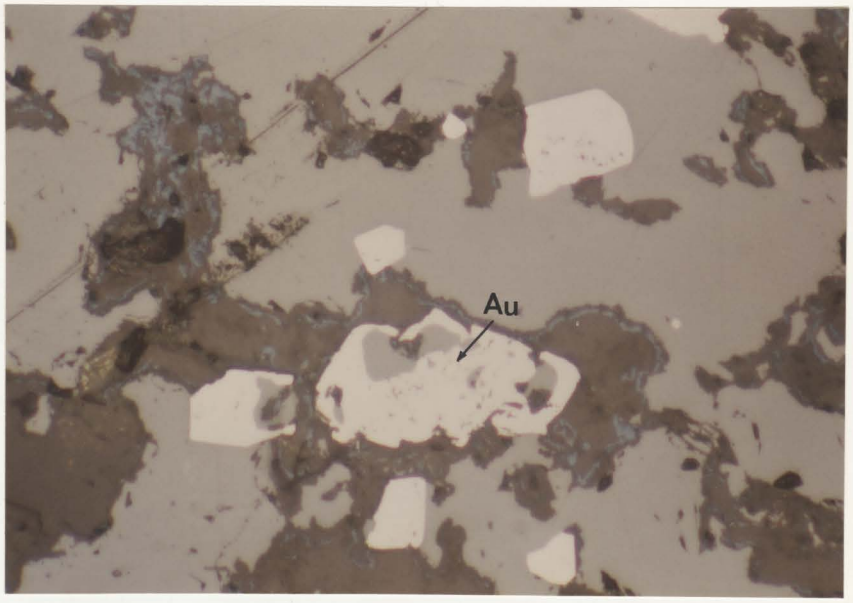
Au

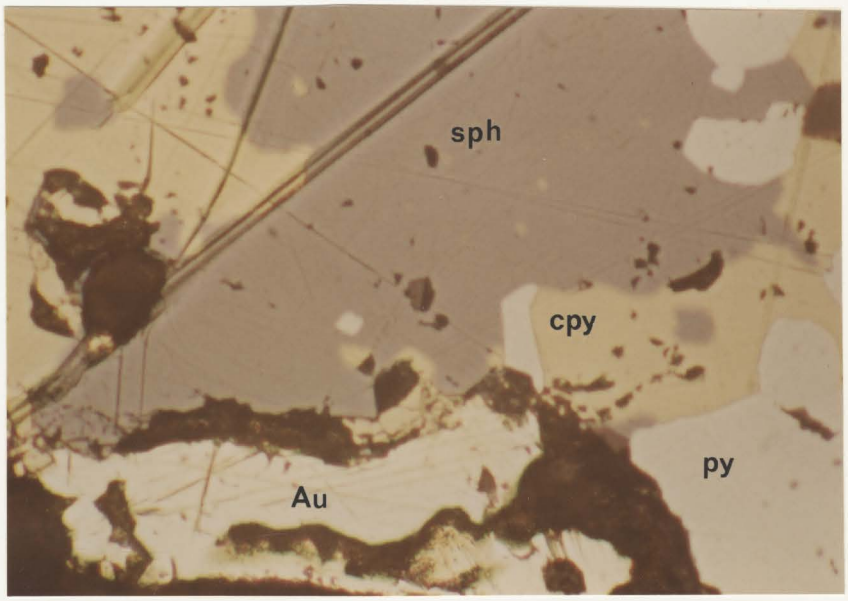
sph
cpy
py
Au

PLATE 35. Gold (Au) in pyrite (py) fracture between sphalerite (sph) and gangue. From sample TDH-36a, "B" horizon. Field of view is 180 μm.

PLATE 36. Gold (Au) filling fracture in pyrite, from sample TDH-44c, "B" horizon. Field of view is 180 μm.

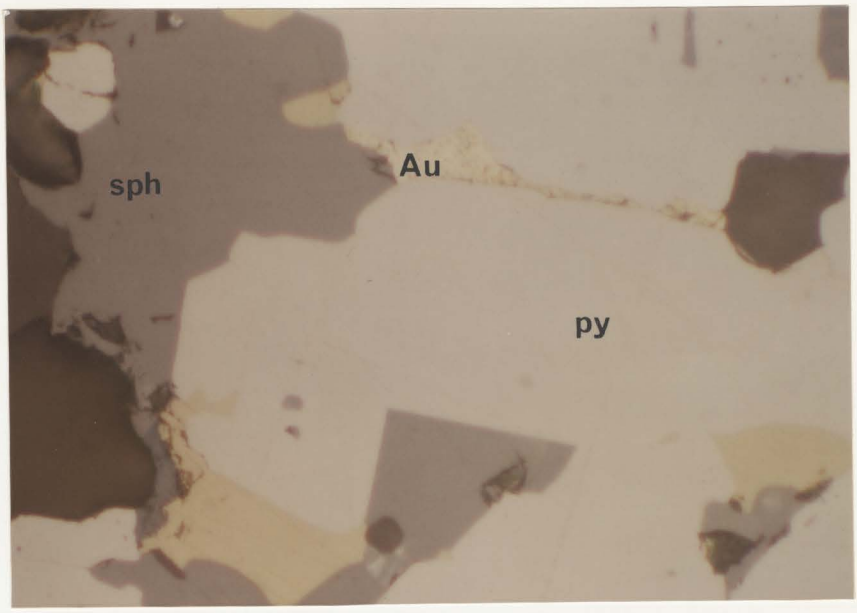
sph
Au
py

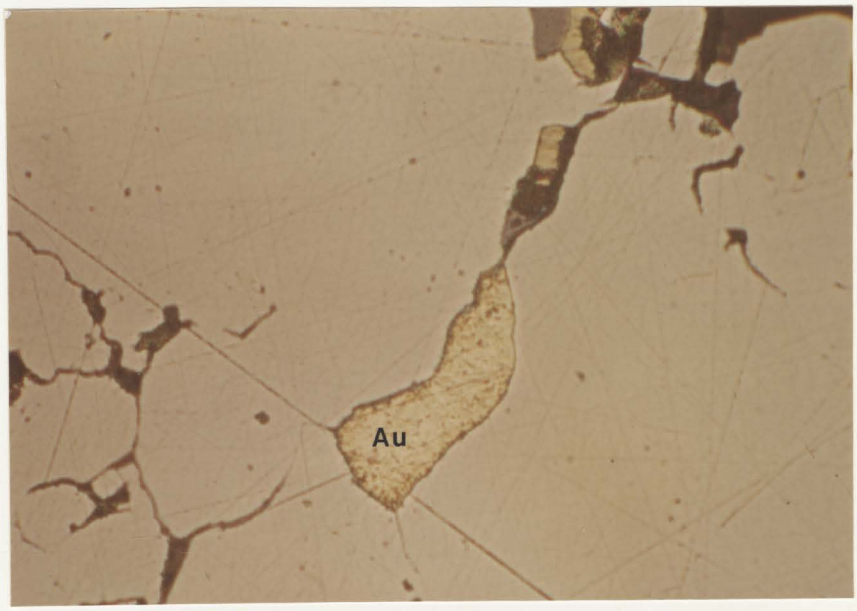
Au

PLATE 37. Gold (Au) cluster in pyrite (py), from sample TDH-38, "B" horizon. Field of view is 1 mm.

PLATE 38. Gold (Au) cluster in pyrite (py), enlargement of Plate 37. From sample TDH-38, "B" horizon. Field of view is 180 μm.

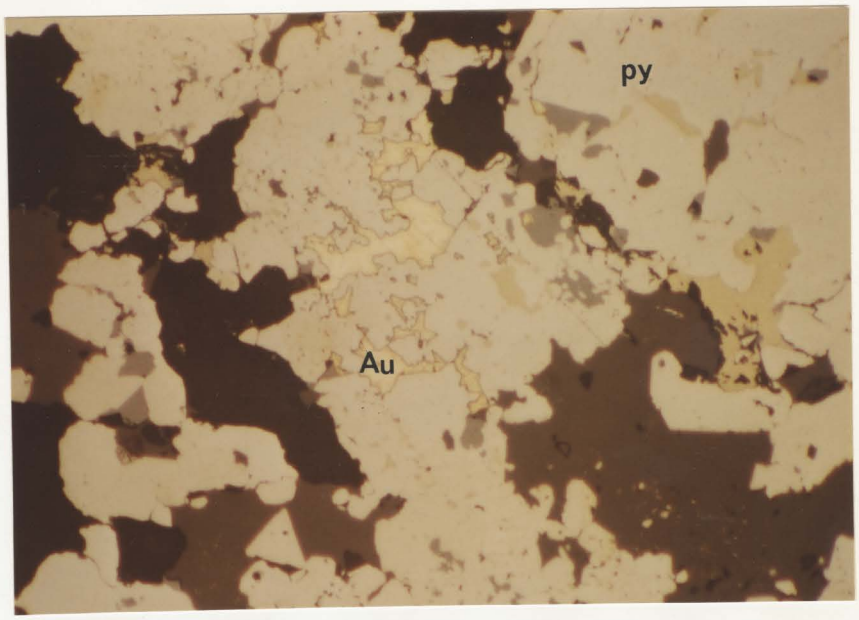
py
Au

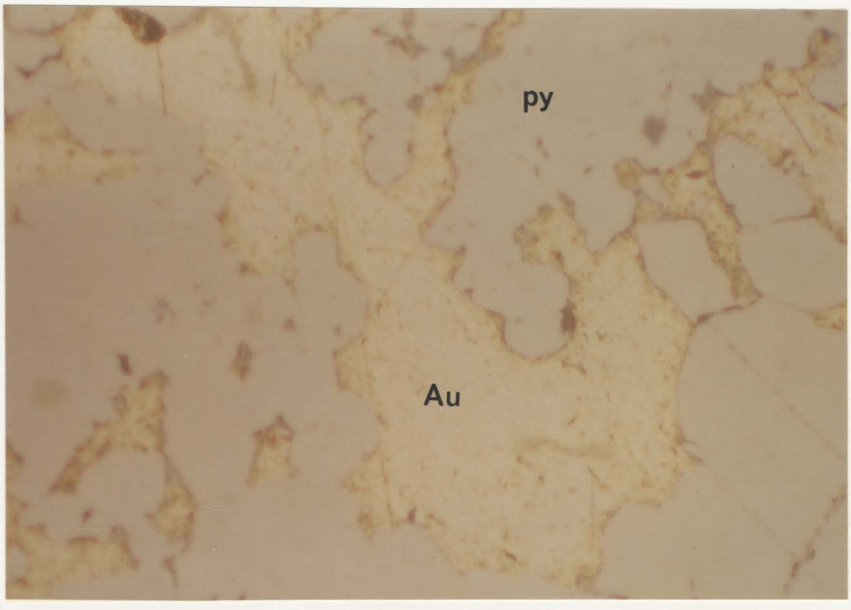
py
Au

PLATE 39. Gold (Au), chalcopyrite (cpy) and sphalerite (gray) in pyrite - atoll texture. From sample sample TDH-18, "B" horizon. Field of view is 180 μm.

PLATE 40. Gold (Au), chacopyrite (cpy) and pyrite (py) in sphalerite (gray). From sample TDH-36a, "B" horizon. Field of view is 180 μm.

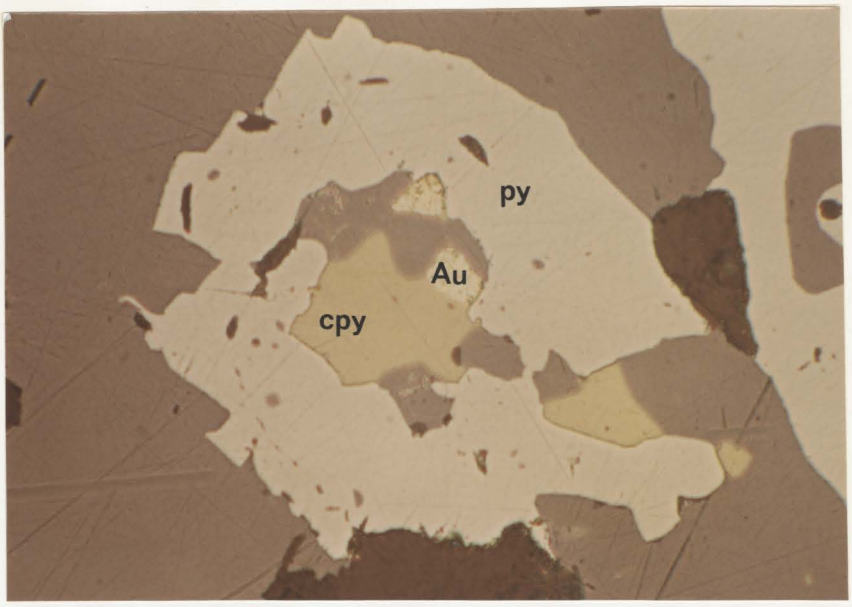
py
Au
cpy

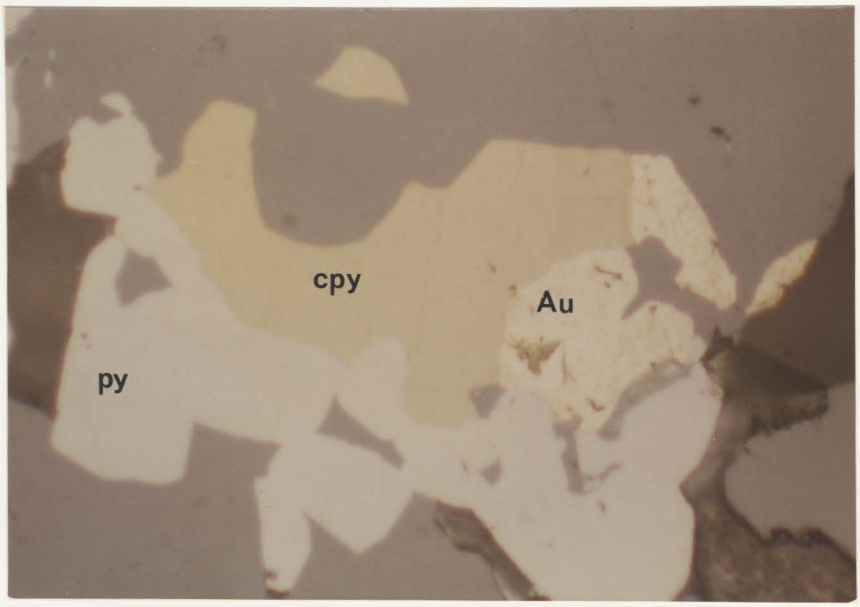
cpy
Au
py

PLATE 41. Gold (as indicated) and sphalerite (gray) in pyrite. Chalcopyrite exsolution in sphalerite (upper right corner). Replacement of cpy and gangue by covellite (blue). From sample TDH-20, "B" horizon. Field of view is .5 mm.

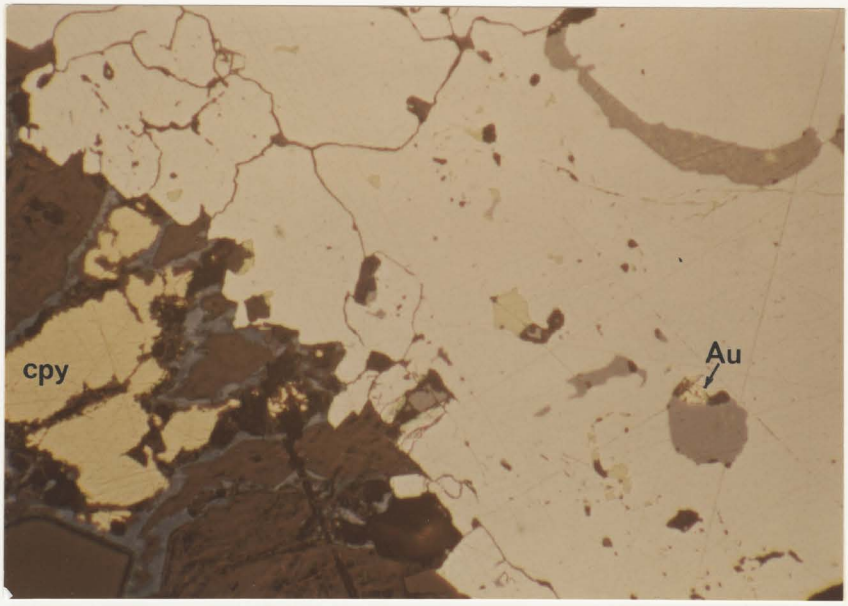
cpy
Au

the pyrite suggesting direct replacement. Most of the gold hosted within pyrite alone is related to fractures. Even where no fracture is seen the overall generality would suggest that minute unseen fractures are present. Though frequently in contact with, gold is rarely hosted by chalcopyrite. Gold hosted entirely by gangue is also uncommon. Of all the gold occurrences examined less than half involved any contact with silicate material. Rare occurrences where gold is found hosted by primary silicates is probably due to direct replacement. In the pyrite-rich sections gold is usually associated with minor chalcopyrite, sphalerite, ± gangue (Plates 31 and 41). In the sphalerite-rich sections gold is often hosted by the sphalerite matrix and frequently in contact with pyrite, chalcopyrite, ± gangue, (Plates 32 and 39).

In Plate 40 the pyrite is being replaced by chalcopyrite which in turn is being replaced by sphalerite and possibly gold. The gold appears to be either contemporaneous with or replacing sphalerite. Plate 35 shows a fleck of gold extending along a fracture in pyrite from sphalerite to a silicate grain. The pyrite has replaced the silicate and is being replaced by the sphalerite. Due to the remobilized nature of the gold through the pyrite, it again appears to be related with the introduction of sphalerite. It is also possible that the gold was in some manner liberated from the silicate, though such a large concentration of gold would be unlikely.

It thus appears that gold is relatively late in the paragenesis though its actual time of emplacement is debatable. In Table I the environments of 36 gold grains from seven polished sections are tabulated. Column one deals with the minerals in direct contact with gold, column two with all minerals in close proximity to gold. Unfortunately the analysis is not very qualitative, though some observations can be drawn. A tally of

Table I

TABULATION OF MINERALS AND MINERAL

ASSEMBLAGES WITH OBSERVED GOLD

Minerals	Au in contact with	Au proximal to
py	1	0
py-fracture	4	0
cpy	1	0
sph	1	0
gangue	2	2
py-cpy	2	0
py-sph	4	6
cpy-sph	2	0
py-gangue	7	9
cpy-gangue	1	1
sph-gangue	1	1
py-cpy-sph	6	11
py-cpy-gangue	2	0
py-sph-gangue	1	0
py-cpy-gangue	0	3
Total gold grains	36	36
% total py	75	89
% total cpy	42	42
% total sph	44	67
% total gangue	42	53

	Average modal % in sections
pyrite	48
chalcopyrite	6
sphalerite	21
gangue	25

the individual minerals in contact with gold reveals pyrite as the most common. Of the 36 gold grains examined, 75% of them had pyrite in direct contact, 42% chalcopyrite, 44% sphalerite and 42% gangue. In the examination of minerals in close proximity to gold (including contact) the pyrite is again most common. Eighty-nine percent of the gold is proximal to pyrite, 42% to chalcopyrite, 67% to sphalerite and 53% to gangue. The lack of increase for chalcopyrite indicates that the mineral has little control in the occurrance of gold. Pyrite and sphalerite increase significantly. The average modal percents of pyrite and sphalerite are approxiamately 48 and 21 respectively. It is possibly due to high modal percentage of pyrite that gold is often found in close proximity to it.

In summary, the gold was probably introduced during replacement of the pyrite (py) and host volcanics by chalcopyrite (cpy) and sphalerite (sph). It often appears to be replacing the chalcopyrite. The relationship with sphalerite is uncertain since evidence for both contemporaneous growth and replacement of sphalerite can be seen. Though the relationship between gold and covellite (cov) cannot be seen directly it is probable that the covellite was introduced later. Remobilization of chalcopyrite, sphalerite and gold alike is evident along fractures. The covellite however does not exhibit such behavior.

A suggested paragenesis for the non-colloform/framboidal "B" horizon ore is as follows: -

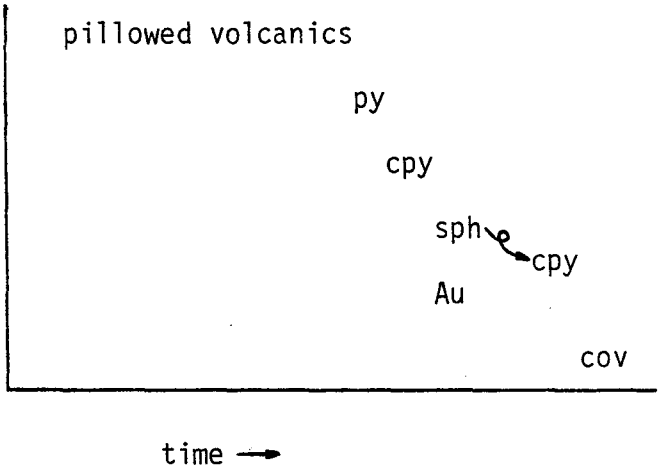

For the colloform/framboidal sections much less replacement is seen. A suggested paragenesis is: -

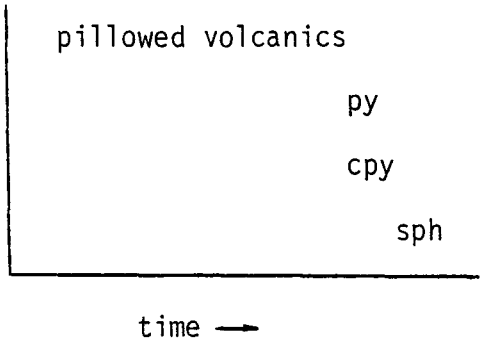

CHAPTER 5

CONCLUSIONS

In the "B" horizon, mineralizing solutions during periods of volcanic hiatus resulted in the deposition of, and replacement of mafic pillowed volcanics by sulphides; pyrite, chalcopyrite and sphalerite with accompanying gold. Mineralization in the East Mine is analogous to that of the "B" horizon in that it is volcanogenic and has resulted in extensive alteration of the footwall rocks. Petrographic observations indicate that the volcanic hosts of both deposits are metamorphically of lower greenschist grade, with a high modal percent of chlorite. The two ore zones differ in geochemistry, mineral textures, and mineral types.

The East Mine volcanics are basaltic komatiitic to magnesium tholeiitic in composition, and alkali depleted. Ore samples from the mine exhibit both replacement textures and well-preserved colloidal textures of pyrite and chalcopyrite. An overall mineral paragenesis for the ores would be: - magnetite → hematite → pyrite → chalcopyrite → sphalerite → covellite, where chalcopyrite occurs contemporaneous with or replaces pyrite.

The "B" horizon volcanics are spillitized magnesium theoleiites. There is no correlation evident in the samples between Au and volatiles, As, Sb, Cu or S. A probable relationship does exist between Au and Zn.

A sphalerite-rich sample containing greater than 40 weight percent Zn exhibited the highest Au value (29 ppm) of the samples analysed. A marked increase in the Au content was noticed in sphalerite separates of two samples. Pyrite and chalcopyrite separates show a decrease in Au content from whole rock values.

The "B" horizon ores host a variety of textures including colloform and framboidal pyrite, exsolution, atoll texture and sulphide banding. The preservation of colloidal pyrite is indicative of very low regional deformation though some local strain features such as cataclastic pyrite are present. Native gold is prevalent in these polished sections. The gold replaces pyrite, chalcopyrite and gangue, and appears to be contemporaneous with sphalerite. An overall paragenesis for the "B" horizon ores would be: - pyrite →chalcopyrite →sphalerite/gold →covellite where chalcopyrite occurs contemporaneous with or replaces pyrite.

The observation of gold in samples from the basal Cape St. John Group ("B" horizon) verifies the results of Kusmirski and Norman (1981) and opens a whole new area to mineral exploration.

REFERENCES CITED

Baird, D.M., 1951, The geology of Burlington Peninsula, Newfoundland Geol. Surv. Canada, Paper 51-21, 70 p.

Chen, T.T., 1978, Colloform and Framboidal Pyrite from the Caribou Deposit, New Brunswick ; Can. Min., 16, p. 9-15.

Church, W.R., 1965, Structural evolution of north east Nfld. - comparison with that of the British Caledonides ; Mar. Sed. 1, no. 3, p. 10-14.

Church, W.R., and Stevens, R.K., 1970, Mantle peridotite and early Paleozoic ophiolite complexes of the Newfoundland Appalachians (abs.) ; Intn. symposium on mechanical properties and processes in the mantle, Intn. Upper Mantle Comm., U.S. Acad. of Sci.

Church, W.R., and Stevens, R.K., 1971, Early Paleozoic ophiolite complexes of the Newfoundland Appalachians as mantle oceanic crust sequences, Jour. Geophys. Res. 76, no.5, p. 1460-1466.

De Grace, J.R., Kean, B.F., Hsu, E., and Green, T., 1976, Geology of the Nippers Harbour map area (2E1B), Newfoundland. Dept. Mines and Energy, Nfld., Rept. 76-3.

Dewey, J.F., and Bird, J.M., 1971, Origin and emplacement of the ophiolite suite : Appalachian ophiolites in Newfoundland. Jour. of Geophysical Res., 76, p. 3179-3206.

Donoghue, H.G. Adams, W.S., and Harper, C.E., 1959, Tilt Cove copper operation of the Maritimes Mining Corp. Ltd. Transactions, Can. Inst. Min. Metal., 42, p. 54-73.

Fyon, J.A., 1980. Seawater alteration of early Precambrian (Archean) volcanic rock and exploration criteria for stratiform gold deposits, Porcupine Camp, Abitibi Greenstone belt, Northeastern Ont. Unpub. M.Sc. thesis, McMaster Univ., Hamilton, 238 p.

Hutchinson, C.S., 1974, Laboratory Handbook of Petro Techniques ; John Wiley and Sons, New York, p. 264-332.

Jenner, G.A., and Fryer, B.J., 1980, Geochemistry of the upper Snorks Arm Group basalts, Burlington Peninsula Newfoundland : evidence against formation in an island arc. Can. Jour. Earth Sci., 17, p. 888-900.

Jensen, L.S., 1976, A New Cation Plot for Classifying Subalkalic Volcanic Rocks ; O.D.M. Misc. Paper 66, 22 p.

Kay, R.W. and Hubbard, N.J., 1978, Trace Elements in Ocean Ridge Basalts ; Earth Planet. Sci. Letters, 38, p. 95-116.

Kusmirski, R.T.M.,1981, Metallogeny of the "East South C" Ore-Zone in the Dickenson Mine, Red Lake, Ontario ; Evidence for Syngenetic Gold Deposition. Unpub. M.Sc. thesis, McMaster Univ., Hamilton, 187 p.

Kusmirski, R.T., and Norman R., 1981, Geology between Tilt Cove and East Pond, East Burlington Peninsula, Newfoundland, incl. 2 maps. Unpub. confidential rept. for Newmont Expl. of Can. Ltd., 61 p.

Manson, V., 1967, Geochemistry of Basaltic Rocks : Major Elements ; in Basalts Vo.1, edited by H.H. Hess and Arie Poldervaart, John Wiley and Sons, New York, p. 215-269.

Marchand, M., 1973, Determination of Rb, Sr, and Rb/Sr by X.R.F. ; Tech. Memo 73-2, Dept. of Geology, McMaster Univ., Hamilton, Ont.

Neale, E.R.W., 1957, Ambiguous intrusive relationship of the Betts Cove - Tilt Cove serpentinite belt, Newfoundland. Proc. Geol. Assoc. Canada, 9, p. 95-107.

Neale, E.R.W., and Kennedy, M.J., 1967, Relationship of the Fleur de Lys Group to younger groups of Burlington Peninsula, Newfoundland. Geol. Assoc. Canada, Spec. Paper 4, p. 139-169.

Neale, E.R.W., Kean, B.F., and Upadhyay, H.D., 1975, Post-ophiolite unconformity, Tilt Cove-Belts Cove area, Newfoundland, Can. Jour. Earth Sci., 12, p. 880-886.

Stanton, R.L., 1972, Ore Petrology ; McGraw-Hill, New York, p. 199-290.

Strong, D.F., 1977, Volcanic regimes of the Newfoundland Appalachians. In : Volcanic regimes in Canada. Edited by W.R.A. Barager, L.C. Coleman, and J.M. Hall. Geol. Assoc. Canada, Spec. Paper 16, p. 62-90.

Strong, D.F., 1980, Geology of the Long Pond - Tilt Cove - Beaver Cove Pond Area, Western Notre Dame Bay, Nfld. ; unpub. confidential Report for Newment Expl. of Can. Ltd., 75 p.

Upadhyay, H.D., 1973, The Betts Cove ophiolite and related rocks of the Snooks Arm Group, Newfoundland. Ph.D. thesis, Memorial University of Newfoundland, St. John's Nfld.

Upadhyay, H.D., Dewey, J.F., and Neale, E.R.W., 1971, The Betts Cove ophiolite complex, Newfoundland : Appalachian oceanic crust and mantle. Proc., Geol. Assoc. Canada, 24, p. 27-34.

Upadhyay, H.D., and Neale E.R.W., 1976, The Betts Cove - Tilt Cove ophiolite and associated rocks, Newfoundland. Geol. Soc. Amer. Abstracts and Programs, North-eastern Section, 8, p. 290.

Williams, H., 1979, Appalachian Orogen in Canada. Can. Jour. Earth Sci., 16, p. 792-807.

APPENDIX A

ANALYTICAL METHODS

A.1. SAMPLE PREPARATION

A representative portion of each sample was crushed in a chipmunk jaw crusher, ground in a disc pulverizer and powdered in a tungsten carbide shatterbox to -200 mesh.

A.2 NEUTRON ACTIVATION

Gold, arsenic and antimony abundances were determined by instrumental (INAA) neutron activation analysis. Approxiamately 0.7 grams of sample powder were weighed into polystyrene vials and irradiated in the McMaster Nuclear Reactor for one megawatt hour along with known chemical standards. After one and a half days of cooling the samples were transported to the lab for counting. Sample preparation and methodology is described in detail by Fyon (1980) and Kusmirski (1981). The Au, As and Sb values are on the order of a few parts per million.

A.3 XRF ANALYSIS OF MAJOR AND TRACE ELEMENTS

Rock compositions were obtained using a Model 1450 AHP automatic sequential x-ray fluorescence spectrometer.

Major elements

Fusion pellets were prepared using the procedure outlined by Hutchinson (1977). A Cr x-ray tube was used to analyse the major elements Si, Al, total Fe, Mg, Ca, Na, K, Ti, Mn and P.

Trace elements

Pressed powder discs were made using the method outlined by Marchand (1973). Trace elements analysed for were Cr, Co, Pb, Cu, Zn, As, V and Ni.

A.4. LECO ANALYSIS

Rock powder samples were analysed for S with the Leco gas analyzer at McMaster University.

A.5. DETERMINATION OF VOLATILES

Loss on ignition (L.O.I.) was determined by heating approxiamately 1.3 g of sample in an electric furnace at 1,000 C for one hour.

APPENDIX B

SAMPLE DESCRIPTIONS

Sample Number	Description and location
TDH- 1	Mafic, variolitic volcanics; hanging wall to "B" horizon.
2	Mafic, variolitic volcanics; hanging wall to "B" horizon.
3	Mafic, variolitic volcanics; hanging wall to "B" horizon.
4	Mafic, variolitic volcanics; hanging wall to "B" horizon.
12	Mafic, variolitic pillowed volcanics; footwall to "B" horizon.
13	Mafic, variolitic pillowed volcanics; footwall to "B" horizon.
14	Mafic, variolitic pillowed volcanics; footwall to "B" horizon.
16	Mafic, variolitic volcanics; Hanging wall to "B" horizon.
22	Mafic, variolitic, pillowed volcanics; footwall to"B" horizon.
43	Mafic, strongly variolitic volcanics; footwall east of "B" horizon.
32	Mafic, variolitic volcanics; hanging wall to "A" horizon.
33	Mafic, variolitic volcanics with disseminated sulphides; hanging wall to "A" horizon.
26	Banded iron formation; "A" horizon.
27	Banded iron formation; "A" horizon.
28	Banded iron formation; "A" horizon.
29	Banded iron formation; "A" horizon.
9	Massive sulphides; "B" horizon.
11	Disseminated sulphides; "B" horizon.
17	Massive sulphides; "B" horizon.
18	Massive sulphides; "B: horizon.
18a	Pyrite + silicate separate of TDH-18.
19	Massive sphalerite; "B: horizon.
19a	Sphalerite separate of TDH-19.
20	Disseminated and massive sulphides; "B" horizon.

44a-f	Disseminated and massive sulphides within pillow; "B" horizon.
38	Massive sulphides (pyrite + sphalerite); fresh "B" horizon.
36ab	Banded sulphides (pyrite + sphalerite); fresh "B" horizon.
34	Chloritized footwall; main lode, East Mine.
35	Weakly mineralized pillow volcanics; picking floor, East Mine.
39	Massive sulphides; float from East Mine.
42	Massive sulphides; float from East Mine.
40	Massive sulphides; float from East Mine.
40a	Chalcopyrite separate of TDH-40.
41	Massive sulphides; float from East Mine.
18b	Pyrite + sphalerite separate of TDH-18.

APPENDIX C

MAJOR AND TRACE ELEMENT

COMPOSITION OF SAMPLES

Table C-1

Sample Number	TDH-1	TDH-2	TDH-3	TDH-4	TDH-12	TDH-13
			In weight %			
SiO_2	49.95	50.40	49.06	50.84	59.03	50.96
Al_2O_3	16.57	16.55	16.34	16.81	15.23	16.62
Fe_2O_3	12.18	12.60	9.78	13.25	9.71	11.99
MgO	10.22	11.20	8.50	10.62	9.21	11.04
CaO	2.44	2.23	6.69	1.35	0.74	1.53
Na_2O	5.05	4.62	5.17	4.69	4.66	4.59
K_2O	<0.20	<0.20	<0.20	<0.20	<0.20	<0.20
TiO_2	0.58	0.58	0.51	1.58	0.55	0.70
MnO	0.33	0.31	0.36	0.28	0.20	0.25
P_2O_5	0.05	0.05	0.06	0.25	0.04	0.06
L.O.I.	4.41	4.40	5.44	3.51	3.22	4.21
Total	101.78	102.94	101.91	103.45	102.59	101.95
			In ppm			
S	42	22	<10	0.27*	340	360
Cr	592	569	505	530	685	515
Co	55	56	36	48	43	47
Pb	15	12	16	35	18	14
Cu	100	41	62	126	124	82
Zn	202	151	193	821	1422	984
V	290	303	237	378	253	304
Ni	175	157	149	155	218	153
As	0.33	0.92	0.71	7.68	1.46	1.46
Sb	0.31	0.68	0.29	0.64	0.21	0.20
Au	0.002	0.008	0.005	0.029	0.010	0.041

* In weight %

Table C-2

Sample Number	TDH-14	TDH-16	TDH-22	TDH-43	TDH-32	TDH-33
			In weight %			
SiO_2	53.19	46.36	48.57	41.48	47.65	N.A.
Al_2O_3	15.59	17.42	17.24	13.43	12.93	N.A.
Fe_2O_3	9.81	14.36	14.92	24.64	10.14	N.A.
MgO	9.95	11.18	11.26	12.23	10.77	N.A.
CaO	4.20	1.82	0.21	0.40	6.09	N.A.
Na_2O	4.40	4.47	4.50	0.99	3.21	N.A.
K_2O	< 0.20	< 0.20	< 0.20	< 0.20	< 0.20	N.A.
TiO_2	0.60	1.03	0.73	0.89	0.28	N.A.
MnO	0.28	0.28	0.26	0.25	1.17	N.A.
P_2O_5	0.06	0.17	0.06	0.31	0.03	N.A.
L.O.I.	4.96	4.51	4.00	5.48	7.96	N.A.
Total	103.04	101.60	101.75	100.74	101.65	25.00
			In ppm			
S	150	N.A.	N.A.	1.49*	24	11.13*
Cr	415	N.A.	N.A.	705	760	331
Co	44	N.A.	N.A.	83	289	122
Pb	< 20	N.A.	N.A.	26	22	< 20
Cu	176	N.A.	N.A.	103	0.37*	13.80*
Zn	557	N.A.	N.A.	0.15*	1.05*	0.07*
V	226	N.A.	N.A.	349	272	171
Ni	166	N.A.	N.A.	286	477	44
As	3.12	0.97	4.16	18.61	1.16	30.24
Sb	0.23	0.44	0.50	1.22	1.01	0.80
Au	0.010	0.005	0.378	0.103	0.044	0.060

* In weight %

N.A. no analysis

Table C-3

Sample Number	TDH-9	TDH-11	TDH-18	TDH-19	TDH-20
			In weight %		
SiO_2	31.49	38.28	32.43	8.11	44.22
Al_2O_3	8.85	10.67	10.82	1.89	9.29
Fe_2O_3	24.04	24.66	28.69	9.16	21.51
MgO	13.48	13.94	16.01	3.06	13.58
CaO	0.07	0.07	0.06	0.07	0.08
Na_2O	0.27	1.09	0.34	< 0.20	1.08
K_2O	< 0.20	< 0.20	< 0.20	< 0.20	< 0.20
TiO_2	0.72	0.69	1.15	0.02	0.74
MnO	0.15	0.18	0.25	0.03	0.18
P_2O_5	0.11	0.08	0.10	0.06	0.09
L.O.I.	N.A.	N.A.	N.A.	N.A.	N.A.
Total	89.18	100.99	119.94	95.66	102.87
			In ppm		
S	9.3*	9.5*	20.0*	29.1*	10.87*
Cr	550	497	506	181	471
Co	76	73	64	21	49
Pb	30	20	62	< 20	40
Cu	0.01*	0.33*	0.46*	0.76*	0.32*
Zn	0.60*	1.50*	9.63*	43.40*	0.91*
V	354	262	235	94	226
Ni	203	217	218	378	196
As	16.47	33.05	N.A.	8.03	49.30
Sb	1.75	1.69	N.A.	1.76	2.39
Au	0.569	2.83	N.A.	28.82	2.32

*In weight %

Table C-4

Sample Number	TDH-44a	TDH-44b	TDH-44c	TDH-38	TDH-40	TDH-41
			In ppm			
S	34.18*	34.66*	N.A.	36.06*	45.98*	35.06*
Cr	275	266	N.A.	362	165	965
Co	132	124	N.A.	65	597	807
Pb	46	49	N.A.	53	35	20
Cu	0.30*	0.30*	N.A.	0.11*	1.54*	0.11*
Zn	0.07*	0.07*	N.A.	0.70*	5.00*	129
V	15	10	N.A.	29	38	119
Ni	123	123	N.A.	18	49	1673
As	23.75	23.39	23.74	79.35	313.21	291.10
Sb	5.15	5.57	5.83	4.85	89.00	14.15
Au	0.487	1.79	0.964	6.87	1.30	0.608

* In weight %

Table C-5

Sample Number	TDH-17	TDH-26	TDH-27	TDH-28	TDH-29
			In ppm		
As	41.59	2.93	9.09	5.22	4.20
Sb	5.04	0.61	0.62	0.60	0.91
Au	8.32	0.473	0.081	0.052	0.074

Table C-6

Sample Number	TDH-18a	TDH-18b	TDH-19a	TDH-40a	TDH-37a	TDH-37b
Mineral Separate	py	sph	sph	cpy	cpy	hem
			In ppm			
As	15.27	59.47	9.51	340.86	1.64	9.71
Sb	1.22	2.28	1.57	50.04	1.62	3.11
Au	1.71	50.32	143.42	0.785	0.081	0.047